

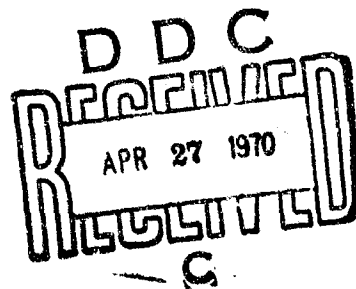
# Measurement and Analysis of Acceleration Environments Generated by NRL Rough Road Simulator

E. W. CLEMENTS

*Ocean Structures Branch  
Ocean Technology Division*

February 1970

AD 704468



Reproduced by the  
CLEARINGHOUSE  
for Federal Scientific & Technical  
Information Springfield Va. 22151

**NAVAL RESEARCH LABORATORY**  
Washington, D.C.

This document has been approved for public release and sale; its distribution is unlimited.

59

## CONTENTS

Abstract	ii
Problem Status	ii
Authorization	ii
List of Figures	iii
References	v
INTRODUCTION	1
Description of NRL Rough Road Simulator	2
MEASUREMENT OF ROUGH ROAD SIMULATOR OUTPUTS	2
Measurement Program	2
Measurement Instrumentation	3
Measurement Procedure	6
ANALYSIS OF ROUGH ROAD SIMULATOR OUTPUTS	6
Analysis Program	6
Analysis Instrumentation	7
Analysis Procedures	8
RESULTS	9
Acceleration Levels	9
Zero-load Spectral Density Data	10
Effect of Load on Spectral Densities	12
Amplitude Distributions	12
CONCLUDING DISCUSSION	13
ACKNOWLEDGMENTS	14

## ABSTRACT

The NRL Rough Road Simulator is a device for determining the resistance of military equipments to damage by the mechanical environments arising from ground transportation. Rough terrain is simulated by presenting a contoured surface moving at controlled speed to the wheels of a tethered vehicle which provides the appropriate mechanical interface between the terrain and the equipment under test. The output motions generated at the machine-equipment interface are of a quasi-random, vibratory nature, and consist of the rigid-body motions of the vehicle and its suspension system and the elastic motions of the vehicle's structure.

The measurement and analysis instrumentation system for such motions must extend the capability of a random vibration instrumentation system to very low frequencies, and in addition possess a high dynamic range capability, since collisions between adjacent structural components of the vehicle may produce local motions of a shock-like nature. A suitable instrumentation system has been assembled, and has provided a representative description of the output motions generated by the Rough Road Simulator and the influence on them of variations in some of the test conditions.

The output motions studied were those produced with a Type M35 6 x 6 truck as the tethered vehicle. Acceleration waveforms were recorded at various points of the truck's cargo space for several equivalent truck speeds, and with dead-weight loads approximating its full rated capacity (5,000 lb), half of rated capacity, and without load. Data are presented in terms of power spectral densities and rms acceleration to permit comparison of the motions at the various locations and to indicate how the motions themselves and the relationships between them are altered by changes in equivalent truck speed and payload.

## PROBLEM STATUS

This is the final report on this phase of the problem.

## PROBLEM AUTHORIZATION

NRL Problem F03-02  
NRL Problem F02-13

Project RR009-03-45-4754  
Project SF013-10-05-11655  
Project SF013-10-05-11658

### List of Figures

1. Schematic of truck cargo space, showing relationship of measurement locations to truck body structure. The positions of the load segments (when used) are shaded.
2. Photograph of the truck cargo space in the full load configuration. The total load is 4522 lb. The transducer package is shown at Location L. Note cutout to permit access to location 32.
3. Block diagram of measurement system. The acceleration channel shown is one of three, the drum speed channel one of two. Acceleration channel calibrations were inserted behind the charge amplifiers, the charge-to-voltage transfer coefficient of the charge amplifiers being checked independently.
4. Block diagram of analysis system.
5. RMS acceleration levels measured at each speed, averaged over all measurement locations. The bars represent the average rms longitudinal component (L), the average transverse component (V), the average vertical component (V), and the average rms resultant of the individual sets of longitudinal, transverse and vertical components (R). A: zero load, B: half load, C: full load.
6. RMS resultant accelerations at each measurement location, averaged for all speeds. RMS resultants are derived as the rms value of the rms accelerations found in the three component directions. The height of the bar plotted at each measurement location is proportional to the average rms resultant acceleration, whose value (in g) is noted at the top of each bar. The average of these values for each row and column are shown by the vertical lines at the ends of the row and column markers. A: zero load, B: half load, C: full load.
7. Vertical component spectral densities at the various measurement locations at an equivalent speed of 5 m/h with zero load. Effective analysis filter bandwidths are: 0.25 Hz, 2-12.5 Hz; 1.25 Hz, 12.5-62.5 Hz; 6.25 Hz, 62.5-300 Hz. A: Loc. 11, B: Loc. 12, C: Loc. 13, D: Loc. 21, E: Loc. 22, F: Loc. 23, G: Loc. 31, H: Loc. 32, I: Loc. 33, J: Loc. 41, K: Loc. 42, L: Loc. 43.
8. Spectral densities of component accelerations at location 23 for speeds of 5, 10 and 20 m/h with zero load. Effective analysis filter bandwidths are: 0.25 Hz, 2-12.5 Hz; 1.25 Hz, 12.5-62.5 Hz; 6.25 Hz, 62.5-300 Hz. A: Longitudinal, 5 m/h; B: Transverse, 5 m/h; C: Vertical, 5 m/h; D: Longitudinal, 10 m/h; E: Transverse, 10 m/h; F: Vertical, 10 m/h; G: Longitudinal, 20 m/h; H: Transverse, 20 m/h; I: Vertical, 20 m/h.

9. Vertical component spectral densities in the vicinity of the load at speeds of 5 and 20 m/h with zero load, half load and full load. Effective analysis filter bandwidths are: 0.25 Hz, 2-12.5 Hz; 1.25 Hz, 12.5-62.5 Hz; 6.25 Hz, 62.5-300 Hz. A: Loc. 22, Zero Load, 5 m/h; B: Loc LL, half load, 5 m/h; C: Loc. L, full load, 5 m/h; D: Loc. 22, zero load, 20 m/h; E. Loc. LL, half load, 20 m/h; F: Loc. L, full load, 20 m/h.

#### References

1. Salter, J.P. and Lee, N.W.L., "The Response of Packaged Military Stores to Truck Transportation - Real and Simulated." R.A.R.D.E. Memorandum 53/65, November 1965.
2. "Road Simulation." Closed Loop, I No. 1, p. 3.
3. "Road Simulator at Dana Fatigue - Tests Cars." Test Engineering, XVI No. 6, p. 32, December 1966.
4. Report of NRL Progress for January 1963, p. 14.
5. Forkois, H.M., "Rough Road Simulator for Wheeled Vehicles," Naval Engineers J., 75 No.5, December 1963, p. 971.
6. Cline, H.T., "Road Shock and Vibration Environment for a Series of Wheeled and Track-Laying Vehicles," Aberdeen Proving Ground Report No. DPS-999, June 1963.
7. Schock, R.W. and Paulson, W.E., "A Survey of Shock and Vibration Environments in the Four Major Modes of Transportation." Shock and Vibration Bulletin No. 35, Part 5, p. 1, February 1966.
8. Forkois, H.M., "Development of a Rough-Road Simulator and Specification for Testing Equipment Transported in Wheeled Vehicles," NRL Report being published.

## INTRODUCTION

Military requirements for electronic (and other) equipments demand reliable operation in spite of a variety of severe environmental conditions. One of the more damaging mechanical environments to which equipments will be subjected arises from handling and transport in combat areas, which may entail hasty loading into any available vehicle followed by rapid progress over assorted unprepared surfaces. One method of testing an equipment's ability to withstand such treatment is to load it into a selected vehicle and transport it about a prepared test track providing a controlled variety of rough surfaces. In addition to its expense and inconvenience, this procedure has the major weakness that the test severity is limited by the motion tolerance of the driver, since a level of severity which seems intolerable on the test track may well be regarded as highly desirable on the battle field. The ability to expose equipments to transportation environments in the testing laboratory by use of an appropriate testing machine is thus a distinct advantage because of the more realistic test severities which may be obtained, as well as allowing transportation testing to be performed in the same facility which performs other mechanical environmental testing. To this end machines have been developed in an attempt to imitate the motion of a vehicle's cargo space. These imitations have little in common with the actuality, although these machines have been useful and provide a reasonable test environment for some types of test package (Ref. 1).

A study group was formed to consider the problem of a more appropriate test machine, and reported favorably on the feasibility of tethering a test vehicle to a device featuring powered bumpy-surfaced drums as a facsimile of rough terrain. Dimensional adjustments would permit a variety of vehicles to be attached and the test severity could be controlled by the speed of rotation of the drums and by adjustment of the profiles of the bumps upon them\*. A machine such as this was constructed and installed at NRL in 1960, and has been described elsewhere (Ref. 4,5).

In order to permit a test procedure to be specified it is necessary that the characteristics of the motions developed in the test vehicles by this machine be known and compared to those found in real life. (Ref. 6,7). The ultimate machine outputs of concern are the cargo space motions of the various vehicles. These outputs will be affected by the nature of the vehicle, its general condition, its load and load reactions, and the point at which motion is measured as well as by the controlled parameters of the test machine itself. It is thus improbable that a given set of operating conditions for the test machine will provide satisfactory outputs for all vehicle, or for a given vehicle with various test packages, or for a given vehicle and test package at different times.

---

\*A more recent approach is to fit long-stroke hydraulic force generators to the wheels of the test vehicle, with the advantage that programming is done electronically (Ref. 2,3).

The motions which must be measured and analyzed are characterized by a more or less random waveform of wide dynamic range and involving components over a broad range of frequencies. Such a motion may be said to be composed of a vibration constituent (due to the suspension, tires, etc.) and a shock constituent (from bumping of structural members, etc.). The instrumentation system used to measure such motions thus must be a hybrid of systems used for either normal shock or vibration waveforms. It must combine the sensitivity and low noise level of a vibration measuring system with the dynamic range and frequency response of a shock measuring system; the system used for analysis requires an even greater range of frequency response than that of most shock analysis systems.

#### Description of the NRL Rough Road Simulator

As installed, the NRL Rough Road Simulator consists of two pairs (right and left) of 33 1/2-in diameter by 30-in wide drive drums and a tethering arrangement. The test vehicle is tethered so that the wheels which underlie its cargo space are supported by the drive drums, any additional wheels simply resting on the floor of the laboratory. The spacing between the fore and aft members of each pair of drive drums may be adjusted to match the spacing of the vehicle's wheels, and, if only two wheels are to be supported, the forward drums of each pair may be uncoupled from the aft by disengaging mechanical clutches. The vehicle used for the studies reported here was a 6 x 6 M-35 truck, so that all four drums were required. In this configuration the forward drums are coupled to the aft by V-belts, and each aft drum is driven (also through V-belts) by an hydraulic motor.

Drum speed is set and controlled by adjusting centrifugal switches on the control console. These are driven directly by flexible shafts from the aft drums, and provide a "bang-bang" type servo loop. The setting of the centrifugal switches gives an indication of nominal drum speed, and variation of actual speed about this setting is indicated by tachometers attached to each of the aft drums. Each drum is fitted with two diametrically opposed profile plates with maximum heights of either 3/4-in or 1 1/2-in. The dynamic loads when the vehicle wheel encounter these bumps lead to variation in the speeds and phase relations of the fore and aft members of each pair of drums, as does normal belt slippage. Similar action leads to speed variation between pairs of drums in addition to that which may be introduced intentionally by means of their independent speed control capability.

#### MEASUREMENT OF ROUGH ROAD SIMULATOR OUTPUTS

##### Measurement Program

The measurement program was devised as a sample of the many possible variations of the operating conditions of the Rough Road Simulator, and

included:

I. Vehicle Variations

- a. Test vehicle: truck, 2 1/2 ton, 6 x 6 M-35
- b. Tire pressure: highway (45 psi)
- c. Load magnitude: empty, one-half rated load and full rated load
- d. Load configuration: dead-weight.

II. Instrumentation Variations

- a. Three components of motion (longitudinal, transverse and vertical)
- b. Measurements at twelve locations within the cargo space of the truck.

III. Machine Variations

- a. Drum speeds equivalent to 5-35 m/h, by increments of 5 m/h.

The motions generated under each combination of these control parameters were recorded for a period of two minutes.

The basic program could be enlarged to include several types of test vehicle, a larger variety of load configurations, and a series of bump profile plates.

Measurement Instrumentation

The measurement locations were selected with an eye to the structure of the M-35 truck serving as a test vehicle, and were arranged in 4 rows and 3 columns (Fig. 1). The first row lay midway between the front of the truck bed and the forward rear axle, the second over the forward rear axle, the third midway between the rear axles, and the fourth midway between the rear axle and the tail gate. The first column lay midway between the left side of the truck bed and the left main chassis rail (and very nearly at the center line of the left dual rear wheels), the second along the center line of the truck bed, and the third over the right main chassis rail. These locations were coded by row number-column number, 11 to 43. Figure 1 also shows the location of the load mounting fixtures (shaded). These were bolted to the truck bed along each of the main chassis rails centered midway between the rear axles, with the right load fixture covering measurement locations 23 and 33. Weights were attached along these fixtures for the half-load runs bringing the total load in the truck to 2316 lb. For the full-load runs, two steel plates were bolted to the fixtures over the half-load weights, bringing the total load to 4522 lb. These plates spanned the space between the load fixtures, and were cut out to permit access to measurement location 32 (Fig. 2).

The transducer package consisted of three piezoelectric accelerometers mounted orthogonally on an insulating block. This was bolted down at each measurement location so that the sensitive axes of the accelerometers were aligned along the length of the truck bed (longitudinal), across its breadth (transverse) and vertically. Since only three accelerometers of appropriate type were available measurements were taken for the various locations sequentially. After conditioning, the accelerometer output signals were recorded on magnetic tape, together with output signals from the two drive drum tachometer generators and a reference (1KHz) sinusoid. Each accelerometer output signal was recorded on two tape tracks, one having twice the gain of the other. A block diagram of the measurement instrumentation system is shown in Fig. 3, and response parameters are listed in Table I.

Table I  
Response Characteristics of Measurement System

Unit	Low-frequency		High-frequency		Low-acceleration		High-acceleration	
	Limit Hz	Hz	Limit kHz	kHz	Limit +g	+g	Limit +g	+g
Accelerometer <sup>1</sup>	.05		4,800		.001		20 <sup>2</sup>	
Charge Amplifier			100,000		.001		20	
Low-pass filter	0		2,500		.001		30	
Tape recorder	0		2,500		.06 <sup>3</sup> .03 <sup>4</sup>		20 10	
Overall system	.05		2,500		.06		20	

1. Natural frequency 12 kHz.
2. Limit for accurate measurement; overloads of several thousand g do not cause damage.
3. RMS noise level, low gain track.
4. RMS noise level, high gain track.

## Measurement Procedure

Measurement runs were performed at each measurement location in sequence, starting at location 11 and proceeding through 12, 13, etc., to conclude at 43. This sequence was completed first without a load in the truck, then with a load of approximately half the rated capacity of the truck, and finally with approximately the full rated load capacity. The procedure followed for each measurement run was to bolt the transducer package in place, adjust the Rough Road Simulator drive drums to an equivalent speed of 5 m/h, and start the magnetic tape recorder. After a two minute period had been recorded, an announcement to this effect was recorded on the tape recorder's voice track, the Rough Road Simulator speed adjusted to 10 m/h, a two-minute sample recorded, and so on in 5 m/h increments of equivalent truck speed up to the maximum obtainable, which was 35 m/h for the unloaded truck and 34 m/h with either half or full load. The master tapes thus include the motions generated when the equivalent truck speed is changing, and speed is indicated by voice markers as well as by drive-drum tachometer outputs.

## ANALYSIS OF ROUGH ROAD SIMULATOR OUTPUTS

### Analysis Program

The resulting records were then processed using an analog (single channel) wave analyzer system with extended low-frequency capability, and utilizing tape-recorder speed-up to achieve the required low frequency response and to shorten the analysis time.

In spite of the playback speed multiplication, analysis requires considerable time. The recordings which were analyzed were selected to provide a cross-section sampling of Rough Road Simulator outputs. In the interests of time conservation, each sample was a 40 second interval taken from the two-minutes-long record, and the analysis performed was well under the maximum capabilities of the analyzer. An analysis of the complete two minutes of data, using the full capabilities (in mode and range) of the analyzer system would require some 50 hours of analysis time for each of the several thousand records.

The initial analysis program thus consisted of:

- a. measurement of rms accelerations for each control parameter combination, and
- b. plotting acceleration spectral density curves and acceleration amplitude distribution functions for several control parameter combinations.

Any future expansion of this basic program could include analysis in terms of Fourier spectra and shock spectra, extension of the frequency range to the full 0.05-2500 Hz obtainable, and processing of each acceleration component at each position at each speed, utilizing the full two minutes of recorded data.

Ideally, the measured waveform should be separated into its shock and vibration constituents, each being analyzed separately, since shock spectra are more appropriate for interpretation of the shock constituent and spectral densities for interpretation of the vibration constituent. While the vibration constituent is associated primarily with the low frequencies and the shock constituent with the high, there is sufficient overlap to prevent their separation by simple filtration.

The distinction between "shock-like" and "vibration-like" constituents in this complex motion is of necessity an arbitrary one. One might say that a typical shock motion is characterized by possessing a sizeable number of frequency components, an amplitude which builds up rapidly from zero to some maximum, then decays more or less rapidly back to zero, and an overall duration which is relatively short: here the terms "rapidly" and "short" are with respect to the dominant frequencies of the motion, and imply that only a few cycles or tens of cycles of the dominant frequencies elapse. A typical vibration motion conversely is characterized by one or a relatively small number of frequency components, an amplitude which does not vary too greatly or too rapidly, and a duration which is long with respect to the dominant frequencies involved. A typical random vibration motion combines some of each of these characteristics. Its frequency components may be many and cover a wide range (or they may not), its amplitude will vary largely and sometimes rather rapidly due to the occasional coincidence of component maxima demanded by the nature of stochastic processes, and its duration is long.

An adequate separation program requires far more elaborate facilities than are available with the present analysis system. Thus for the data obtained here there has been minimal attempt to differentiate between shock and random vibration.

#### Analysis Instrumentation

The magnetic tape recorder had a dual-tape capability allowing it to transport 1/2 in. and 1 in. wide tape simultaneously. Head patching permitted the recorded signal to be played back from the 1 in. master reel and recorded on a 1/2 in. analysis loop. Little signal degradation was incurred, since re-recording was in the predetection mode and time correlation was assured by driving both tapes with the same capstan. The analysis loop then furnished a repetitive signal to the wave analyzer, distribution function analyzer and voltmeter.

The wave analyzer was an electronically swept heterodyne type having analysis filter bandwidths of .5, 2, 10 and 50 Hz, and a square law detector. The distribution function analyzer had a precision manual control for level selection and provided a meter deflection indicating the percentage of time this level was exceeded or not exceeded by the input signal's instantaneous value; a plot of this meter reading vs level control setting is thus representative of the amplitude cumulative distribution function of the input signal. The voltmeter was a true RMS type with a bandwidth of 2Hz - 200 KHz. Figure 4 shows a block diagram of the analysis system.

### Analysis Procedure

Since it was apparent that only a sampling of records could be handled in a reasonable length of time, the most informative sample should be chosen. Survey of the literature and observation of the Rough Road Simulator in operation indicated that the frequency range of 2-300 Hz is likely to contain most of the significant components in these records, and the vertical acceleration component is the strongest, usually by a considerable margin. The speeds of 5 and 10 m/h are the most desirable speeds in terms of driver toleration, and some speed will be the most severe in terms of rms acceleration.

Preliminary analysis consisted of measuring the rms acceleration levels from all of the records obtained. The results of this substantiated the above observations and pin-pointed the most severe speed at 20 m/h. Spectral densities were measured for the following selected group of records: in the zero load condition, the vertical acceleration components at each measurement location for speeds of 5, 10 and 20 m/h, and in addition the transverse and longitudinal components at measurement locations 23, 32 and 41 for the same speeds; in the half-load condition, the vertical acceleration components at measurement locations 43 and LL (left load segment) for speeds of 5 and 20 m/h, and in the full load condition, vertical components at locations 43 and L (load plate) for speeds of 5 and 20 m/h. Amplitude distributions were also measured for these records while the spectral density analysis was in progress. While sparse, this selection is sufficient to indicate the variations in spectral properties due to the variables of geometry, orientation, load and speed.

The time required to frequency-analyze a single record was much reduced by playing the analysis loop at 60 1/s, which multiplied the frequencies involved by a factor of 8 and shortened the duration of the record by the same factor, since the original recording was made at 7.5 1/s. The higher frequency permitted broader analysis filters to be used without loss of resolution, and the much faster scan rates thus permitted results in a large reduction of the total analysis time even though the scan range is larger by a factor of 8. Further

reductions in analysis time resulted from switching to broader analysis filters when the scan reached an appropriate frequency, and proceeding at a faster scan rate than otherwise permissible.

Using the speeded-up play-back, the wave analyzer program was to scan from 16-100 Hz with the 2 Hz filter, 100-500 Hz with the 10 Hz filter, and 500-2400 Hz with the 50 Hz filter, yielding a worst-case resolution of 12.5%. Analysis time was further reduced by analyzing the first 40 seconds of the two minute record, providing a worst-case sampling error estimate of +25%, with 80% confidence. Analysis uncertainty was reduced by empirically determining the maximum scan rate consistent with build-up time for each filter. The final program required 2 1/2 hours for analysis of each record.

Since it was not feasible to separate the shock and vibration constituents of the recorded waveforms, it was essential to retain the highest possible dynamic range. Accordingly, the low-gain tape records were analyzed, and amplifier gains set to provide maximum permissible levels for an input corresponding to the 20 g maximum capacity of these tape channels. Careful balancing and other adjustments permitted the noise level to be reduced to 34 db down from the maximum level (with square law detection) so that signal-to-noise ratio was not unduly impaired.

The spectral density plots consequently represent signal samples which may contain some constituents of a shock nature. With the voltmeter and distribution function meter it is possible to recognize when a probable shock transient appears and to compensate for it, tending to restrict the rms levels and distribution functions to the vibratory part of the signal. This tendency for the spectral density plots to represent a different aspect of the motion is much reduced by the greatly longer effective averaging time of the wave analyzer as compared to the other two instruments.

## RESULTS

### Acceleration Levels

Figure 5 shows the variation of rms acceleration components with equivalent truck speed, averaged over all measurement locations. The acceleration components are represented by the bars labelled L (longitudinal), T (transverse), and V (vertical); the additional bars labelled R (resultant) are the rms values of the rms components. Figure 6 shows the rms resultant acceleration at each measurement position, averaged over all truck speeds. The basal plane in Fig. 6 represents the cargo space of the truck, and the loads and measurement locations are shown in approximately their actual positions. Numbers at the top

of each bar give the resultant acceleration at that position in g rms; the height of the bar is proportional to this quantity. Vertical lines at the ends of rows and columns give average resultants for those rows and columns.

Figure 5 indicates that the most severe speed (on the average) is 20 m/h, largely because the truck becomes increasingly airborne at the higher speeds. The effect of increasing load is to reduce the acceleration levels induced and to hold the truck down on the machine until somewhat higher speeds are reached, so that for the full-load condition the severity at 25 m/h is no less than that at 20 m/h. It may also be seen that the vertical acceleration component is the largest by a substantial margin.

Figure 6 shows the general lowering of resultant acceleration levels throughout the cargo space due to adding load. As might be expected, the accelerations measured directly on the load weights are low, and those at locations removed from the neighborhood of the load fixture are not much affected by the presence of the load. The highest levels are generally found across the fourth row, and the lowest across the third.

#### Zero Load Spectral Density Data

Spectral densities were obtained for data measured at all positions and speeds, for the zero load condition. However only a representative sampling is included here. Figure 7 presents the spectral densities (in  $g^2/Hz$ ) of the vertical accelerations at each position of the truck cargo space at a drum speed of 5 m/h. The spectral densities of the vertical accelerations have most of the continuum concentrated below 20 Hz, while the higher frequencies are represented by a relatively few line components. This pattern is typical for all speeds, components and positions. One of the more striking features is the very strong 46 Hz component at location 23, which evidently contributes much to the high rms levels of Figs. 5 and 6. Interestingly, this component is not apparent at locations 13 or 33, but there is a fairly strong 58 Hz component at location 43. While the vicinity of 60 Hz is an unsettling place to find a strong component, it is accompanied by lesser components at 170 Hz and 240 Hz, all of which show normal growth with increasing speed, and which do not appear at other locations. It is evidently real. The data from locations 13 and 33, on the other hand, show well defined component bands in the sub-20 Hz region.

Recalling the placement of measurement locations, it might be expected that column 3 would show the most beam-like behavior (as it lies along the right main chassis rail), column 2 to be most like a set of plates, and column 1 somewhere intermediate. By and large this seems to be borne out. Column 3 appears most frequency-selective and most position-dependent, column 2 most broad-banded in frequency,

and least position dependent, and column 1 is somewhere in between.

At 10 m/h all positions show some discrete band structures in the region below 20 Hz. While the overall level is higher, the higher frequency components increase more than the low frequency continuum, tending to fill in the spaces between the line components and leading to a more continuous spectrum in this higher-frequency region.

At 20 m/h, the higher frequency components are stronger and more nearly continuous. However, the low frequency region does not reach much higher levels. Instead, the effect seems to have become one of filling in the noles between the bands noted in Fig. 7. The components just above 2 Hz now seem to be the most important in the sub-20 Hz region.

Figure 8 gives the spectra/density data for the three acceleration components measured at location 23 for speeds of 5, 10 and 10 m/h. The longitudinal and transverse components show the same spectral growth and filling-in as previously remarked in the vertical component. The strong 46 Hz component in the vertical spectrum is also quite respectable in the other directions, but the dominant 160 Hz component of the longitudinal motion is fairly small in the vertical, and only slightly larger in the transverse direction. It may also be noted that the lowest frequencies do not dominate the sub-20 Hz region of the longitudinal and transverse spectra as they do the vertical. The peaks in this region lie around 5-8 Hz for these directions, rather than the frequency of 2 + Hz of the vertical. It is possible, of course, that additional peaks lie below the range of analysis, but it is unlikely that these would greatly exceed those plotted, as the energy contained in the plotted components accounts for the measured rms levels reasonably well.

The component spectra at location 32, which lies along the center of the truck's cargo space midway between the axles and is about the "softest" of the measurement position, show that high frequency components are quite weak, and almost completely absent in the transverse direction. A low band centered about 48 Hz in the vertical and a 280 Hz line observable in the longitudinal finally appear in the transverse, but a 190 Hz line noticeable in the others does not appear. Only in the longitudinal direction do the high frequency components compare with the strength of those in the region below 20 Hz.

At location 41, also, the high frequency components are less pronounced than the low; the dominant high frequency lines being at 56 Hz in the vertical direction (also prominent in the longitudinal), 140 Hz in the transverse (also visible in the other two directions) and 280 Hz

in the longitudinal (also detectable in transverse and vertical). Again, the lowest frequencies scanned seem more influential in the vertical direction than in the others, although additional peaks may lurk undetected beyond the analysis range.

One may epitomize the spectral densities observed as being composed of three distinct elements: (1) a low frequency continuum, relating primarily to the motion input to the truck, while increases in level and shifts to higher frequencies as speed increases; (2) a low frequency line structure associated with the truck's suspension, tires, etc., which is little affected by change in speed; (3) a high frequency line structure representing the structural response of the truck's cargo space, which is strongly increased in level by increasing speed.

#### Effect of Load on Spectral Densities

Figure 9 shows the variation of acceleration spectral densities measured in the region of the load as a result of increasing load for two speeds. The measurement locations were (1) for the full-load condition, the load itself (the lowest acceleration position), (2) for the half-load condition, the left load segment (also the lowest acceleration position), and (3) for the zero load condition, location 22 (closest to the other two, although not the lowest acceleration location). The speeds considered are 5 m/h (the least severe) and 20 m/h (the most severe).

From Fig. 9 it appears that the reduction in acceleration level as load is increased is due largely to suppression of the truck bed's structural modes. While these vanish, the peak spectral densities in the low-frequency region associated with the suspension, etc., remain essentially unchanged; the energy in this region becomes concentrated in fewer, better defined modes and shifts to lower frequencies. Increase in speed, at any given load, seems to provide the same general changes in the spectral pattern, namely to shift the low-frequency segment to somewhat higher frequencies and slightly increase its line components and to strongly increase such high frequency segment as may be present. A particular effect of speed which does vary with load is the behavior of that part of the spectrum referred to as the low frequency continuum, which increases in level when the truck is not loaded but does not when it is.

#### Amplitude Distributions

While spectral density analyses were in progress, the signal samples were also fed into a cumulative distribution analyzer. Signals were normalized to provide the same rms voltage input, and an attempt was made to restrict the signals to those of a vibratory

nature. The differences between curves due to load, speed, etc., are smaller than the uncertainties, and the departure from normality surprisingly small, save for the extremities. This will not be the case, of course, if the entire motion, involving shock transients, is considered.

#### CONCLUDING DISCUSSION

The system of components assembled for the measurement and analysis of low level, very low frequency, quasi-random accelerations has been found well suited to its purpose, and has considerably more capability than has been exploited by the shake-down reported here. It may be said that the practical limit to the analysis procedure is set by the amount of time feasible to spend, rather than by limitations of the analyzer system. While some mechanical inconveniences exist in the operational procedure, they are slight and can be removed by minor updating of some system components.

It is not practicable at this time to relate the motions generated by the test vehicle on the Rough Road Simulator with those generated by this type of vehicle on a rough road. "Rough Road" constitutes an elusive concept, as testified by the profusion of test courses maintained at such places as Aberdeen Proving Ground. While some measurements of the motions undergone by this type of vehicle on various test tracks have been made, little information is available in published form. In view of the random nature of the motion, it is not likely (nor is it necessary) that the motion waveforms produced by a test machine would correspond to those produced by actual terrain. Such a correspondence would in fact be more likely to be a detriment, as the simulation would then be highly specific, and any test would lack the universal applicability desired in an environmental test.

Reference (6) provides some data for motional parameters of this type of vehicle travelling on test tracks; from the only spectral density plot included it appears that the Rough Road Simulator has only a crude resemblance to the APG cross-country course. Whether it resembles one of the other test courses more closely remains unknown. What is ultimately desired in a laboratory test machine is to be able to attach a specimen item to it in a specified way, to operate the test machine in a specified way, and to conclude, if the item survives, that one is x% confident it will survive transportation in any vehicle over any terrain y% of the time. This requires knowledge of the envelope of actual transportation environments which is not available, and hence it is not possible to do so.

#### ACKNOWLEDGMENTS

The author would like to express his thanks to H. M. Forkois, C. L. Lamb, P. Pida, and E. A. Stephanoff, who made the Rough Road Simulator available for gathering the data for this project, designed and installed the loading arrangements, and operated the Rough Road Simulator to the requirements of the measurement program.

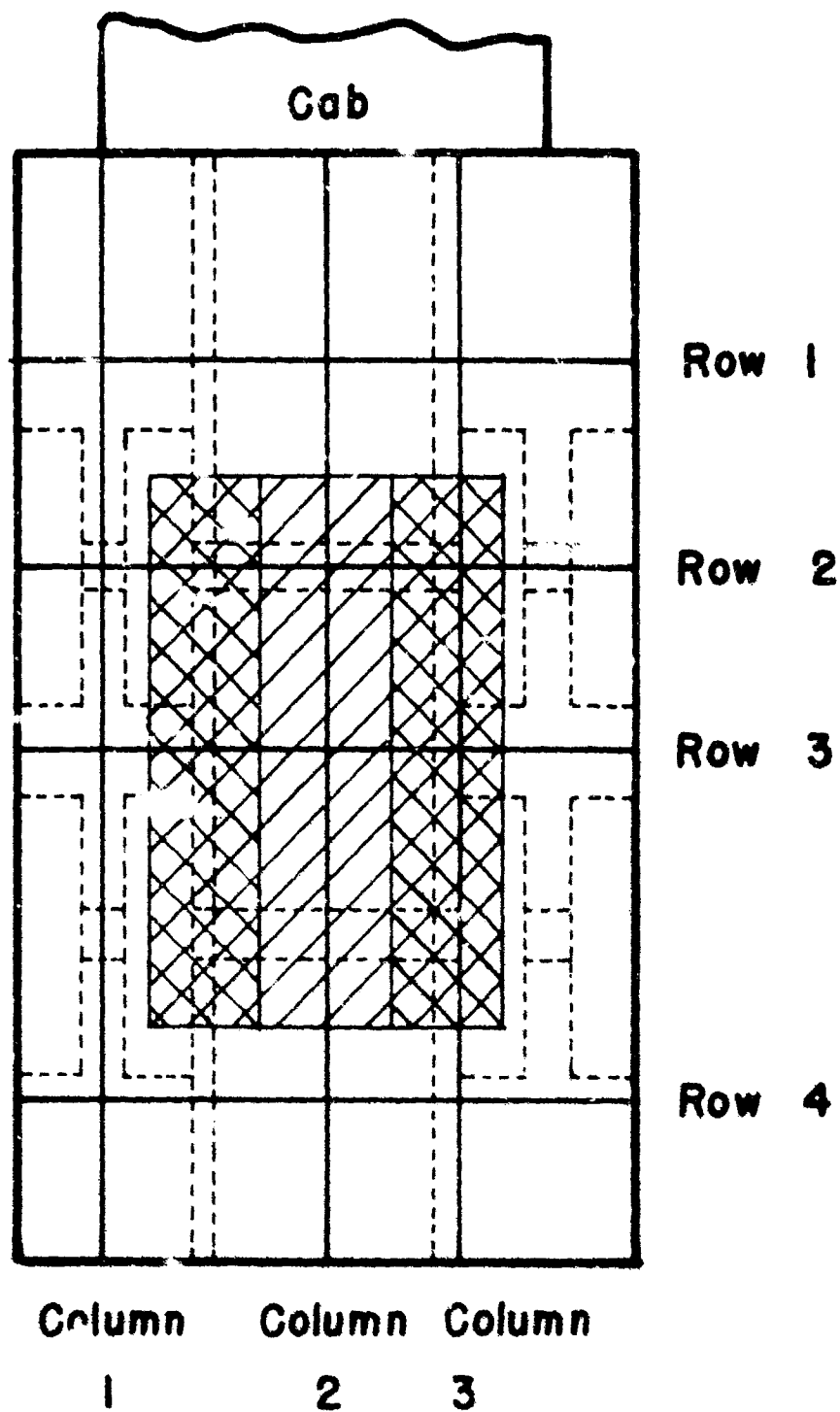


Fig. 1 - Schematic of truck cargo space, showing relationship of measurement locations to truck body structure. The positions of the load segments (when used) are shaded.



Fig. 2 - Photograph of the truck cargo space in the full load configuration. The total load is 4522 lb. The transducer package is shown at location L. Note cut-out to permit access to location 32.

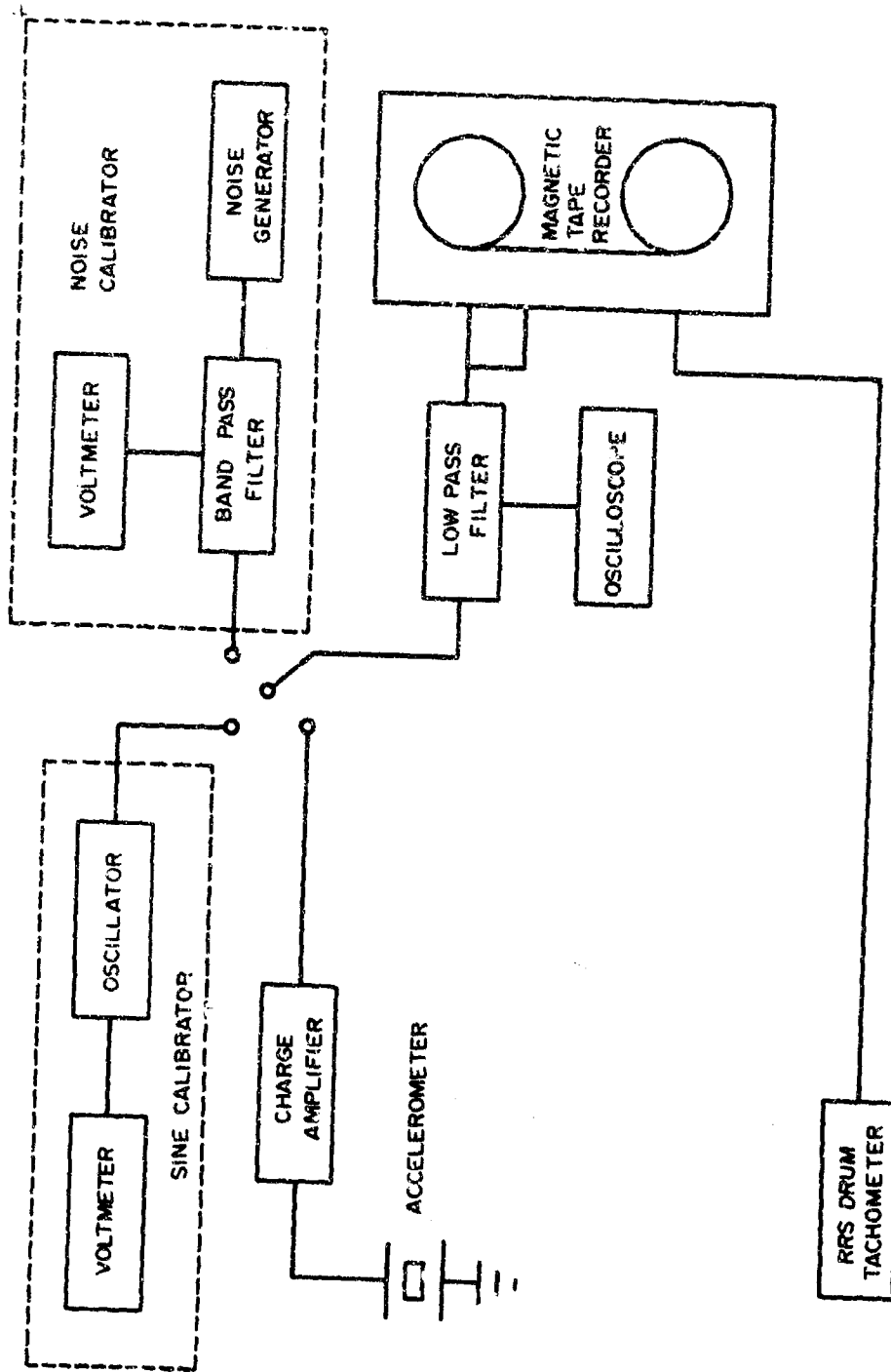


Fig. 3 - Block diagram of measurement system. The acceleration channel shown is one of three, the drum speed channel one of two. Acceleration channel calibrations were inserted behind the charge amplifiers, the charge-to-voltage transfer coefficient of the charge amplifiers being checked independently.

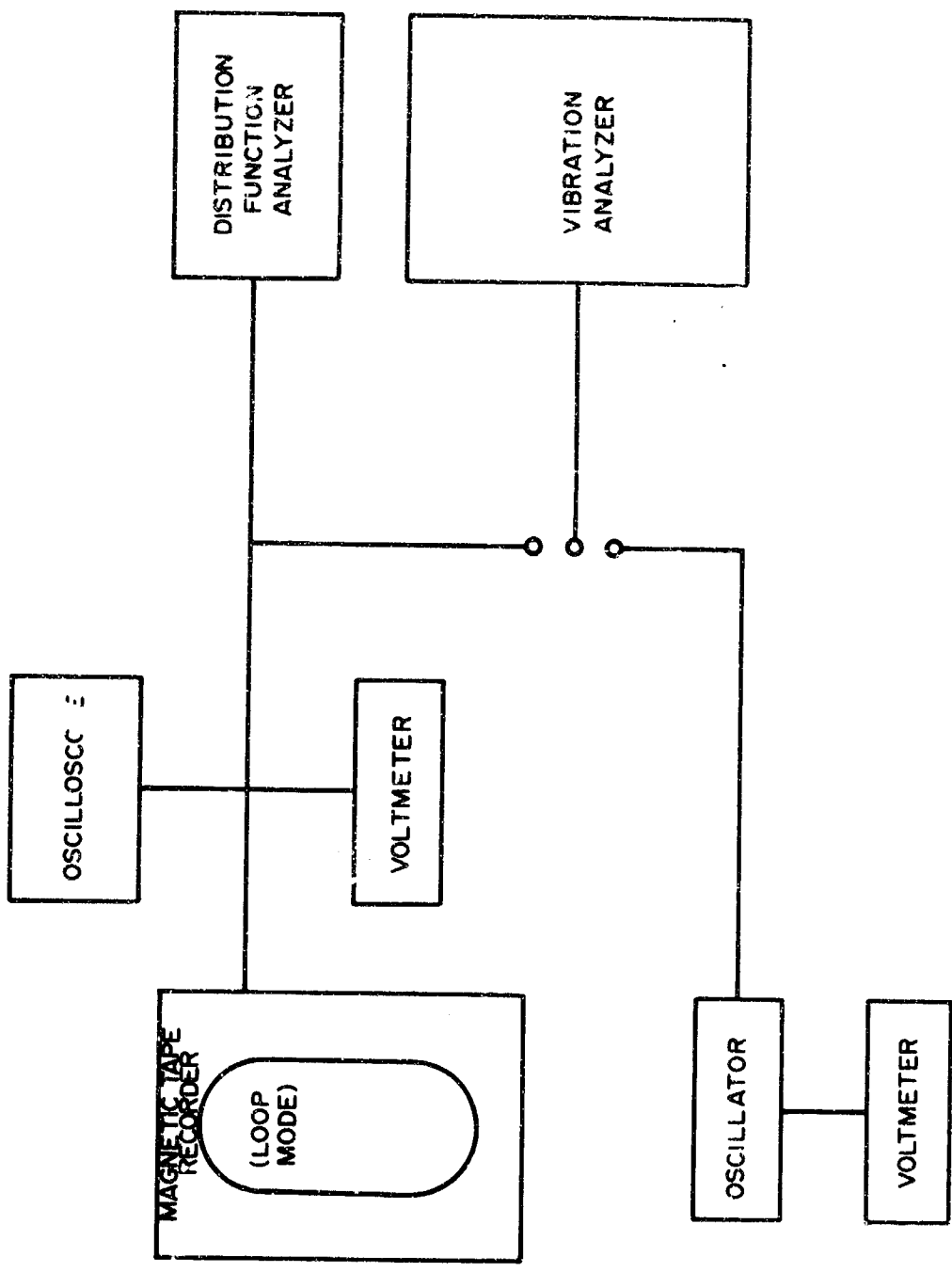


Fig. 4 - Block diagram of analysis system

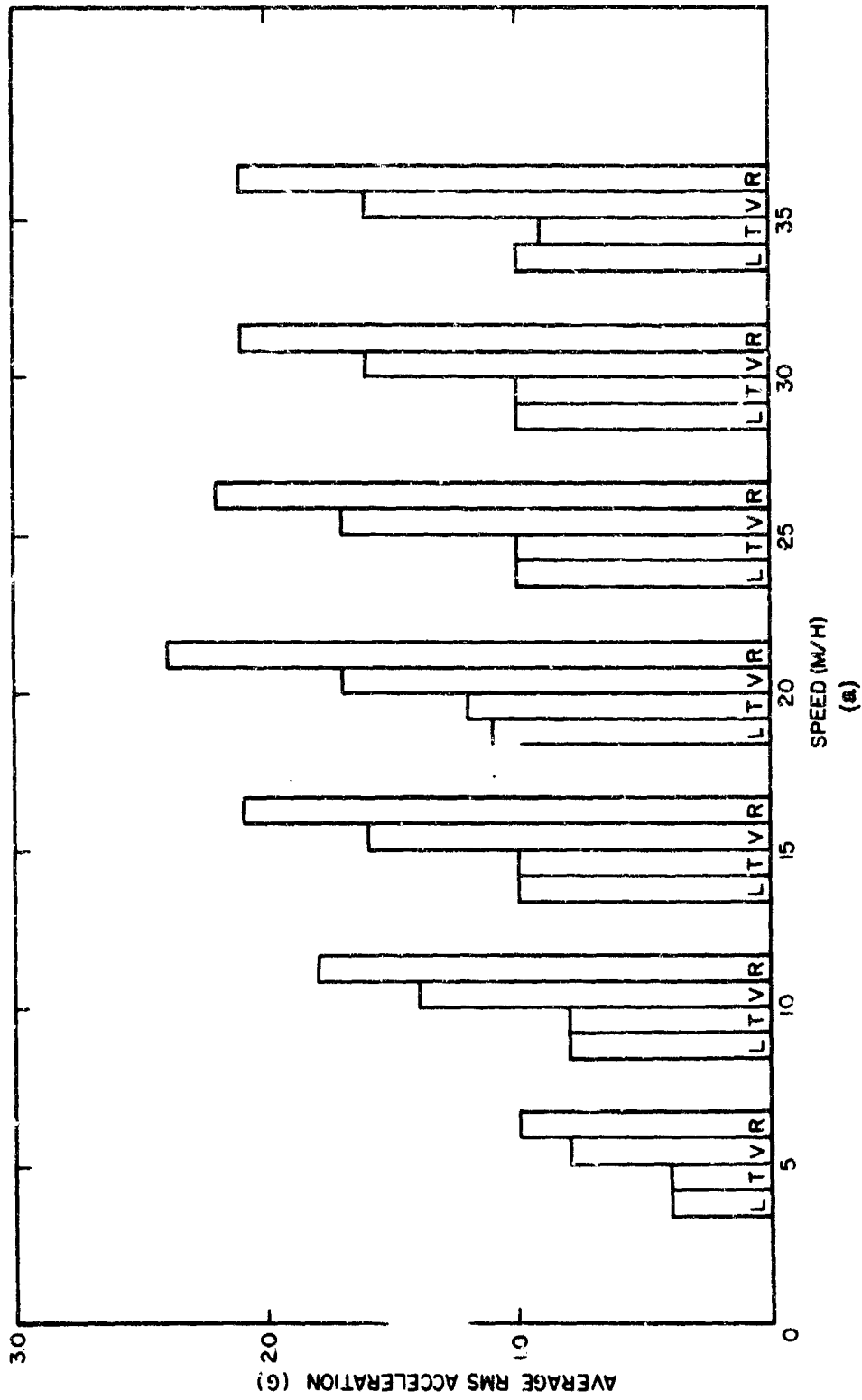


Fig. 5 - RMS acceleration levels measured at each speed, averaged over all measurement locations. The bars represent the average rms longitudinal component (L), the average transverse component (T), the average vertical component (V), and the average rms resultant of the individual sets of longitudinal, transverse and vertical components (R). A: zero load, B: half load, C: full load.

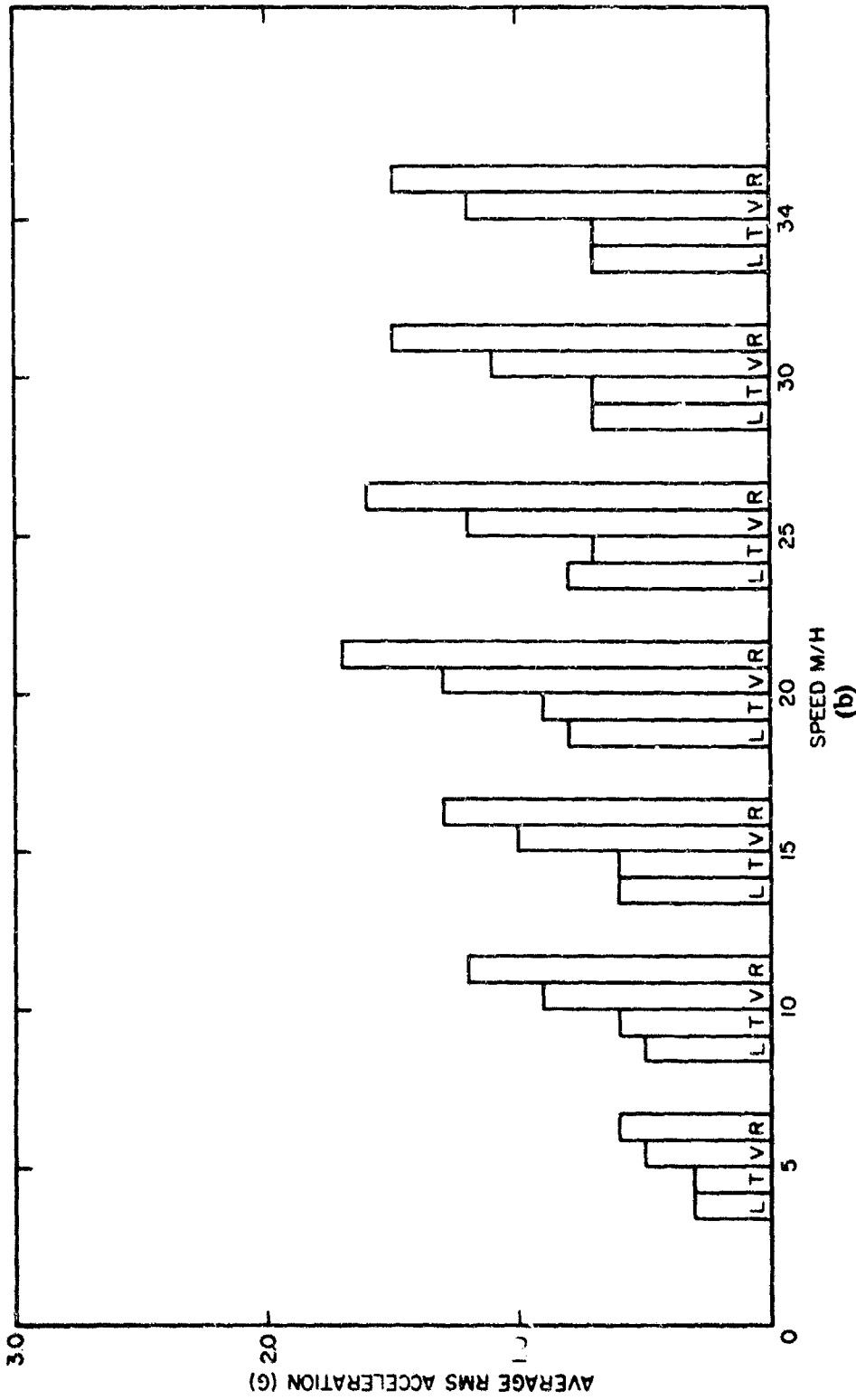
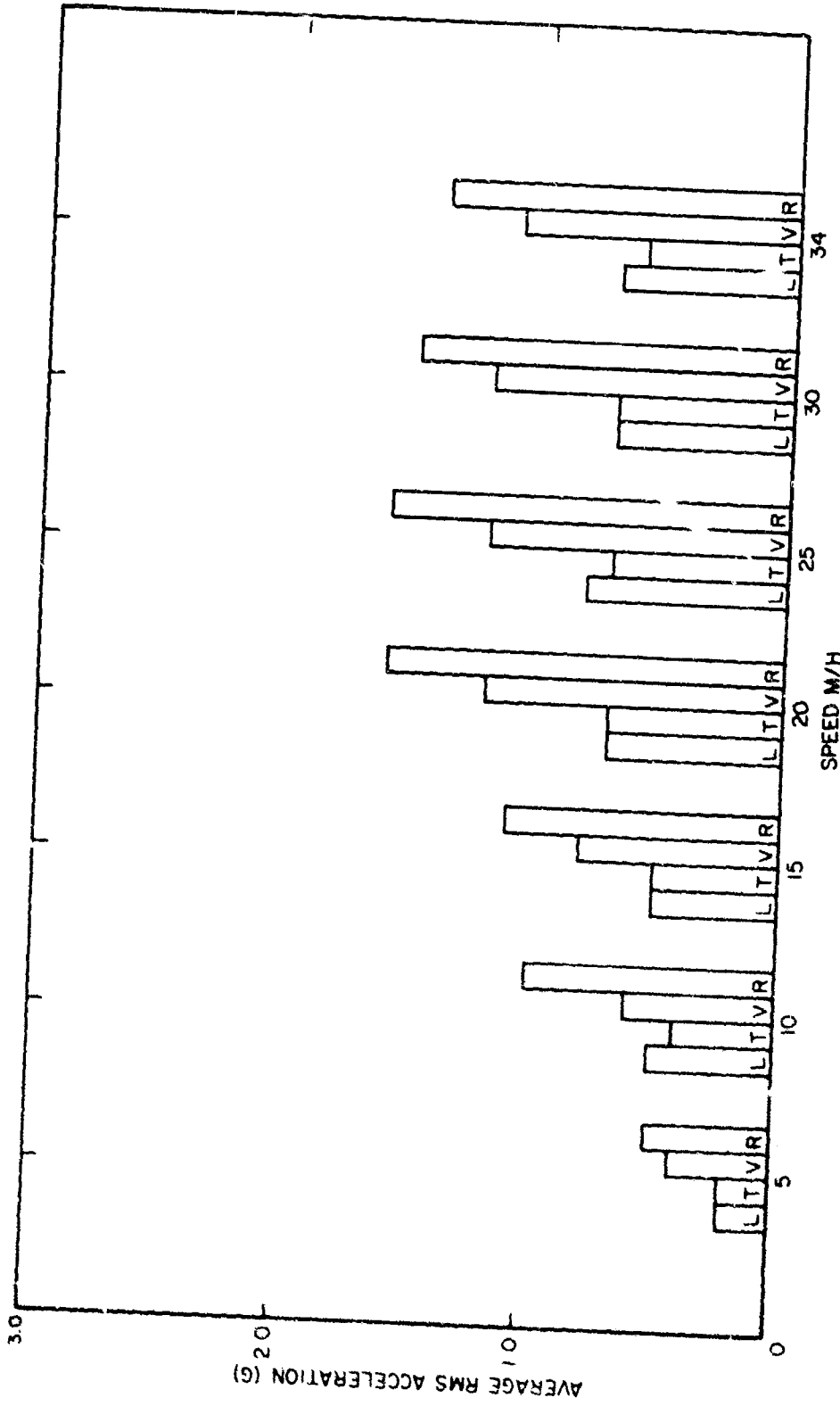
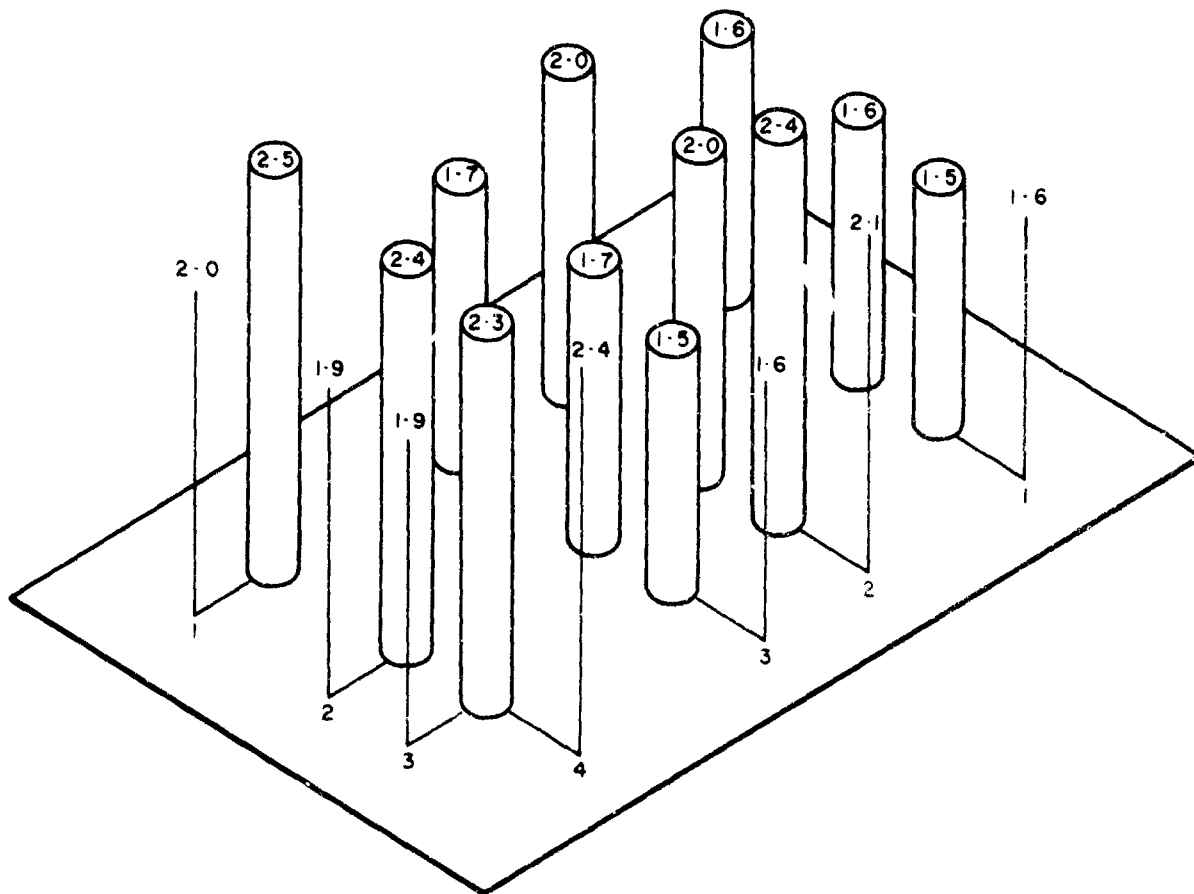


Fig. 5 (cont'd) - RMS acceleration levels measured at each speed, averaged over all measurement locations. The bars represent the average rms longitudinal component (L), the average transverse component (T), the average vertical component (V), and the average rms resultant of the individual sets of longitudinal, transverse and vertical components (R). A: zero load, B: half load, C: full load.

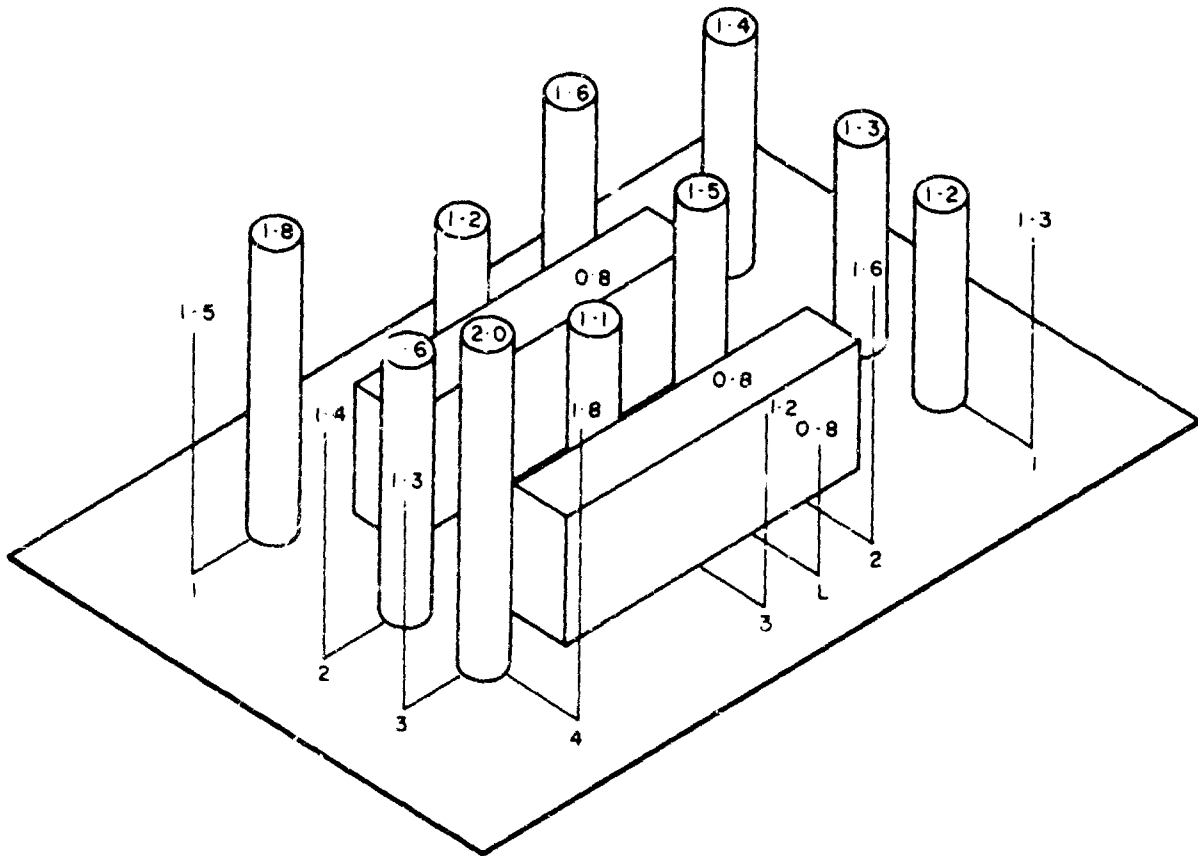


(c)  
 Fig. 5 (cont'd) - RMS acceleration levels measured at each speed, averaged over all measurement location. The bars represent the average rms longitudinal component (L), the average transverse component (T), the average vertical component (V), and the average rms resultant of the individual sets of longitudinal, transverse and vertical components (R). A: zero load, B: half load, C: full load.



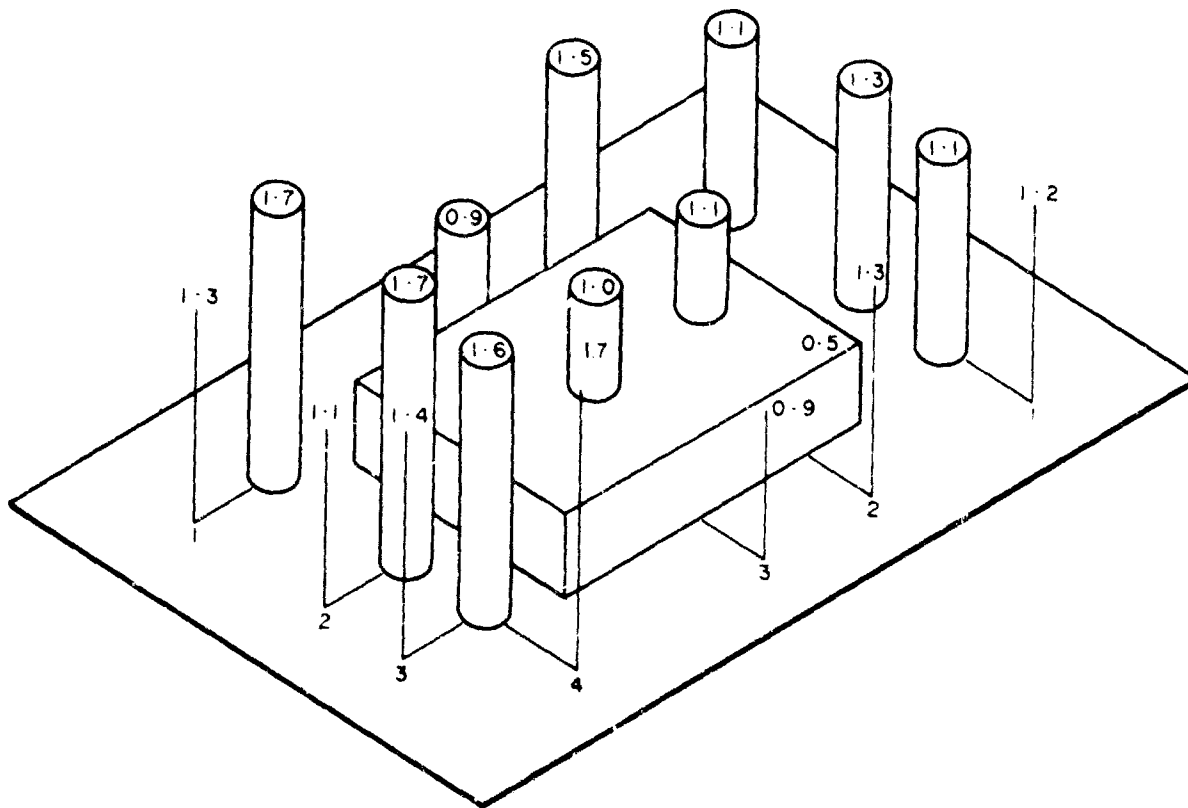
(a)

Fig. 6 - RMS resultant accelerations at each measurement location, averaged for all speeds. RMS resultants are derived as the rms value of the rms accelerations found in the three component directions. The height of the bar plotted at each measurement location is proportional to the average rms resultant acceleration, whose value (in g) is noted at the top of each bar. The average of these values for each row and column are shown by the vertical lines at the ends of the row and column markers. A: zero load, B: half load, C: full load.



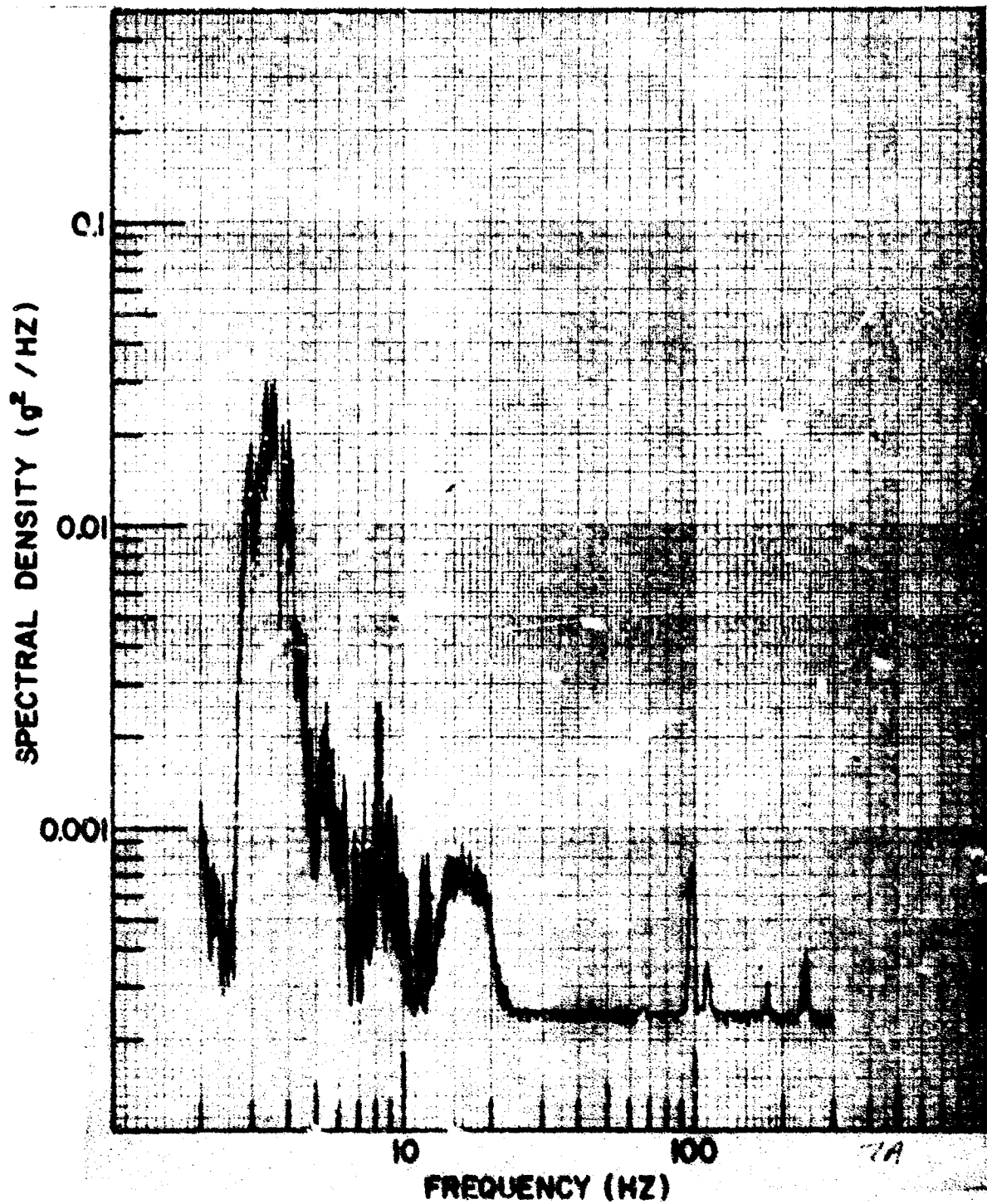
(b)

Fig. 6 (cont'd) - RMS resultant accelerations at each measurement location, averaged for all speeds. RMS resultants are derived as the rms value of the rms accelerations found in the three component directions. The height of the bar plotted at each measurement location is proportional to the average rms resultant acceleration, whose value (in g) is noted at the top of each bar. The average of these values for each row and column are shown by the vertical lines at the ends of the row and column markers. A: zero load, B: half load, C: full load.



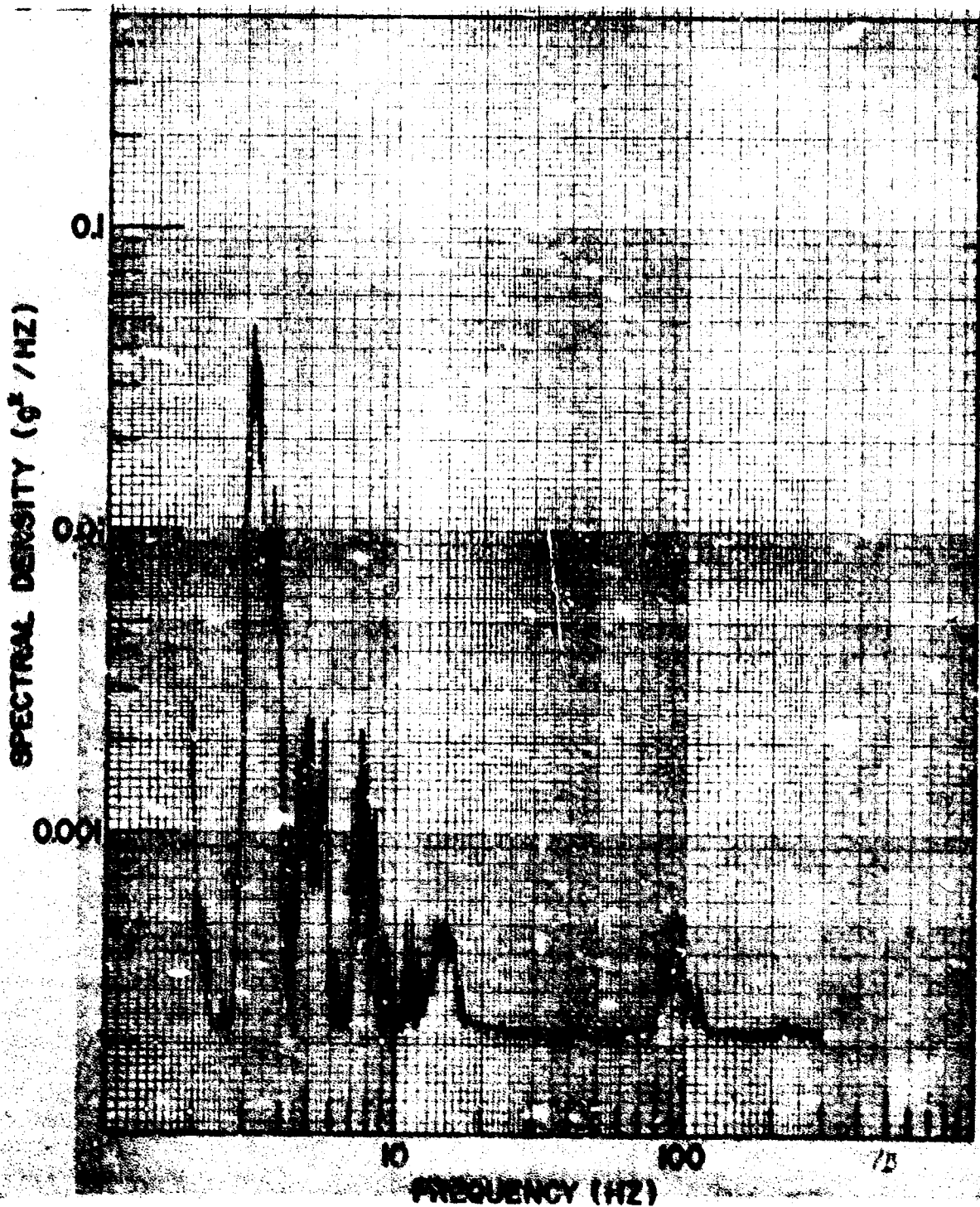
(c)

Fig. 6 (cont'd) - RMS resultant accelerations at each measurement location, averaged for all speeds. RMS resultants are derived as the rms value of the rms accelerations found in the three component directions. The height of the bar plotted at each measurement location is proportional to the average rms resultant acceleration, whose value (in g) is noted at the top of each bar. The average of these values for each row and column are shown by the vertical lines at the ends of the row and column markers. A: zero load, B: half load, C: full load.



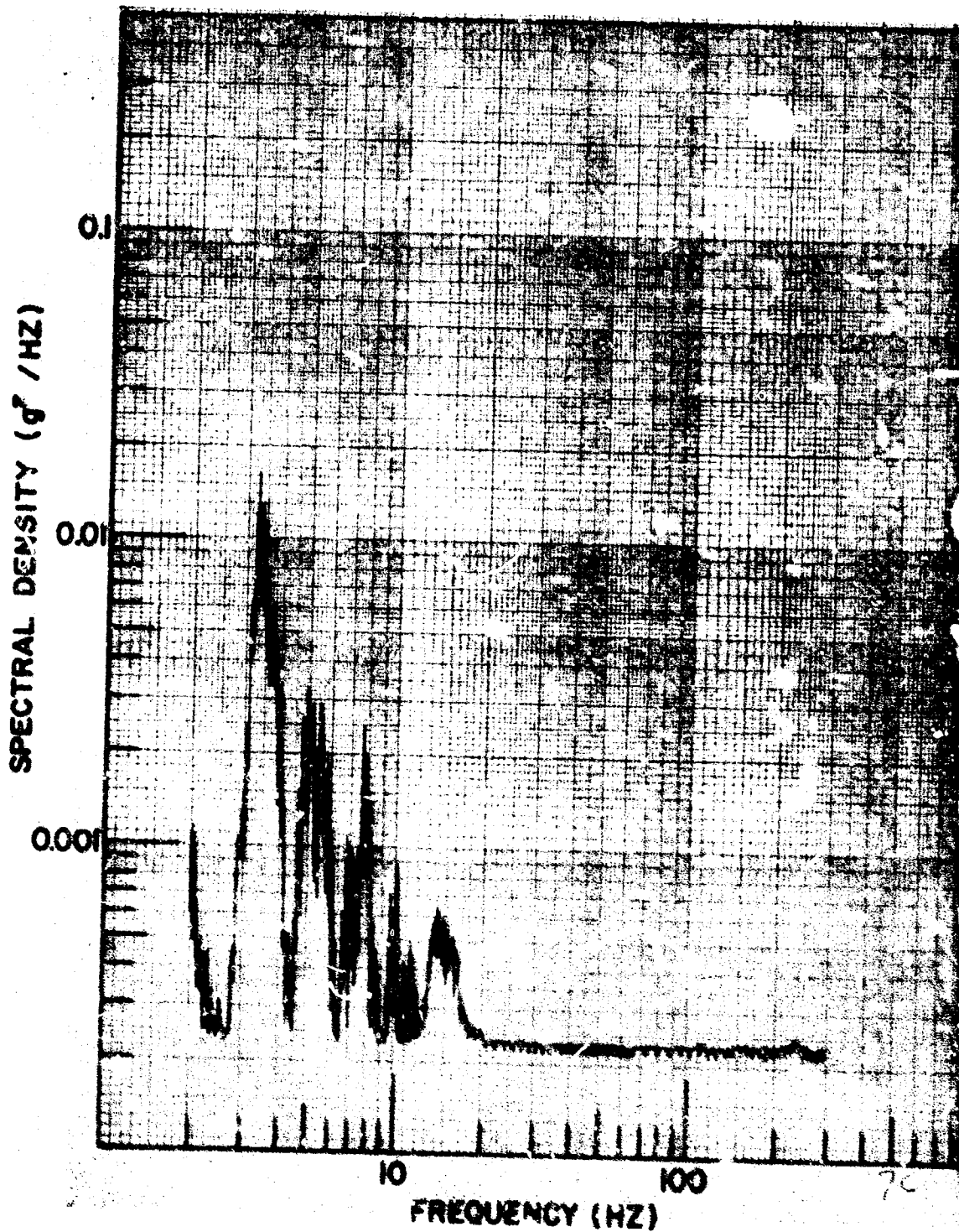
(a)

Fig. 7 - Vertical component spectral densities at the various measurement locations at an equivalent speed of 5 m/h with zero load. Effective analysis filter bandwidths are: 0.25 Hz, 2-12.5 Hz; 1.25 Hz, 12.5 -62.5 Hz, 6.25 Hz, 62.5-300 Hz. A: Loc. 11, B: Loc. 12, C: Loc. 13, D: Loc. 21, E: Loc. 22, F: Loc. 23, G: Loc. 31, H: Loc. 32, I: Loc. 33, J: Loc. 41 K: Loc. 42, L: Loc. 43.



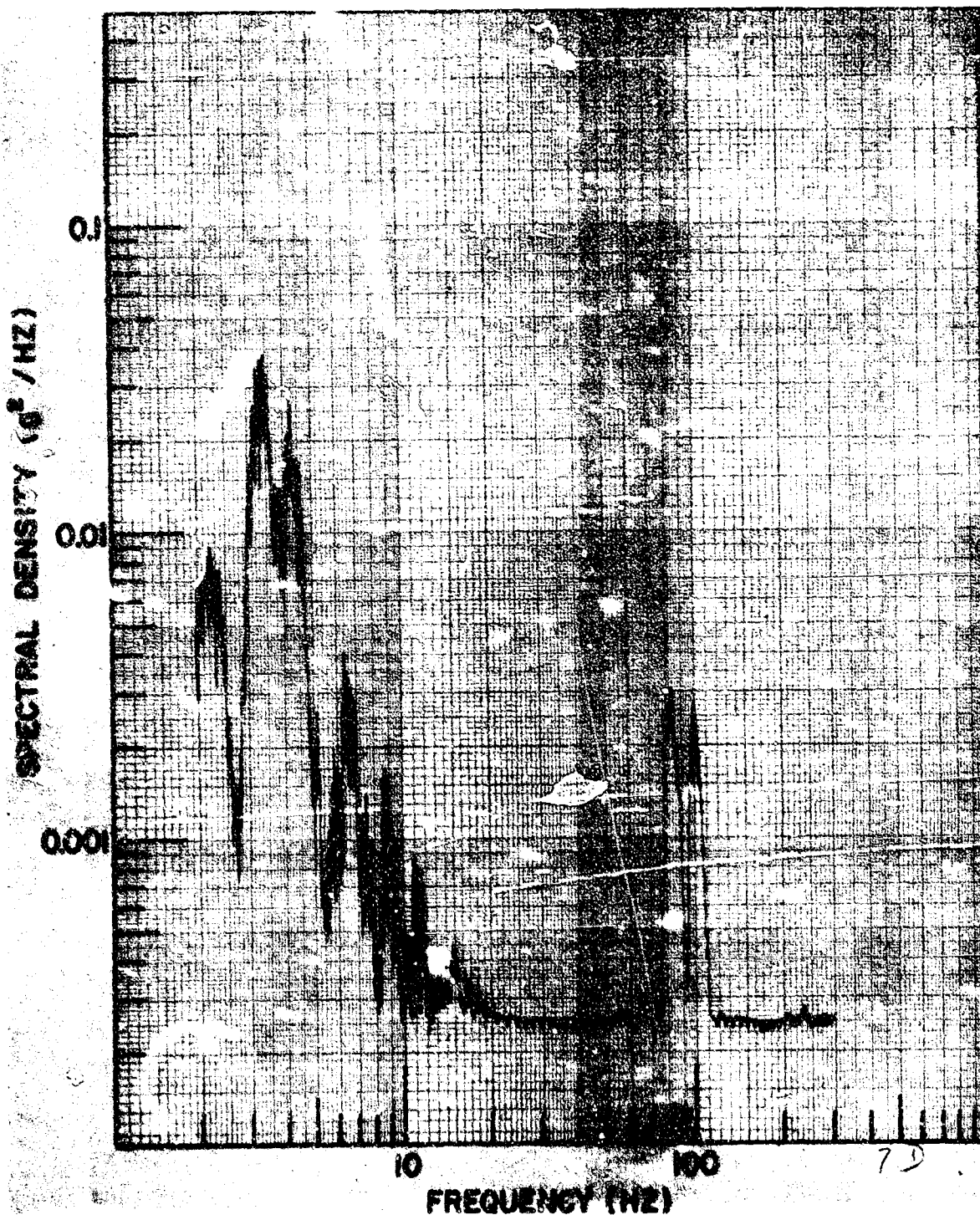
(b)

Fig. 7 (cont'd) - Vertical component spectral densities at the various measurement locations at an equivalent speed of 5 m/h with zero load. Effective analysis filter bandwidths are: 0.25 Hz, 2-12.5 Hz; 1.25 Hz, 12.5-62.5 Hz; 6.25 Hz, 62.5-300 Hz. A: Loc. 11, B: Loc. 12, C: Loc. 13, D: Loc. 21, E: Loc. 22, F: Loc. 23, G: Loc. 31, H: Loc. 32, I: Loc. 33, J: Loc. 41, K: Loc. 42, L: Loc. 43.



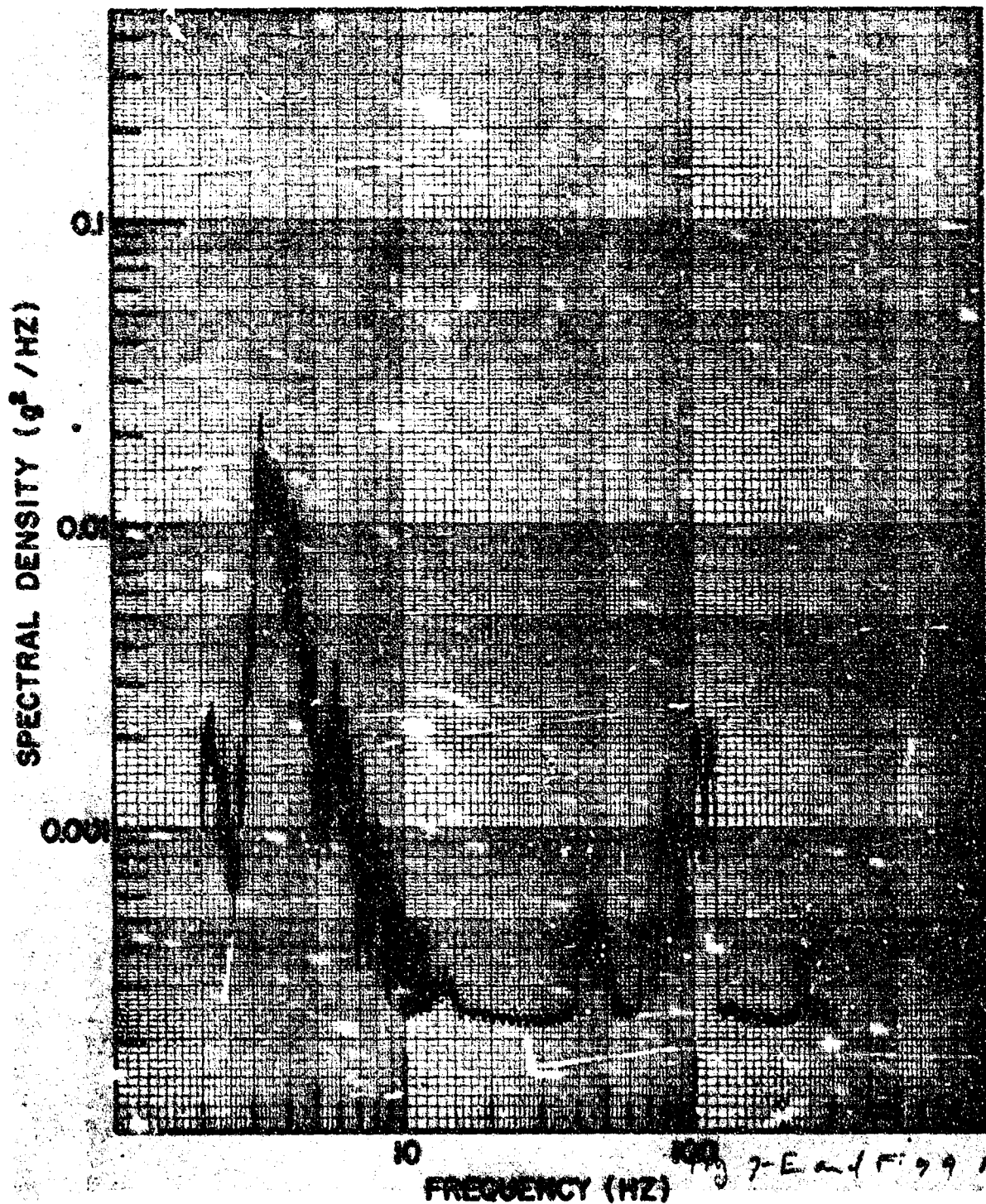
(c)

Fig. 7 (cont'd) - Vertical component spectral densities at the various measurement locations at an equivalent speed of 5 m/s with zero load. Effective analysis filter bandwidths are: 0.25 Hz, 2-12.5 Hz; 1.25 Hz, 12.5-62.5 Hz, 6.25 Hz, 62.5-300 Hz. / Loc. 11, B: Loc. 12, C: Loc. 13, D: Loc. 21, E: Loc. 22, F: Loc. 23, G: Loc. 31, H: Loc. 32, I: Loc. 33, J: Loc. 41, K: Loc. 42, L: Loc. 43.



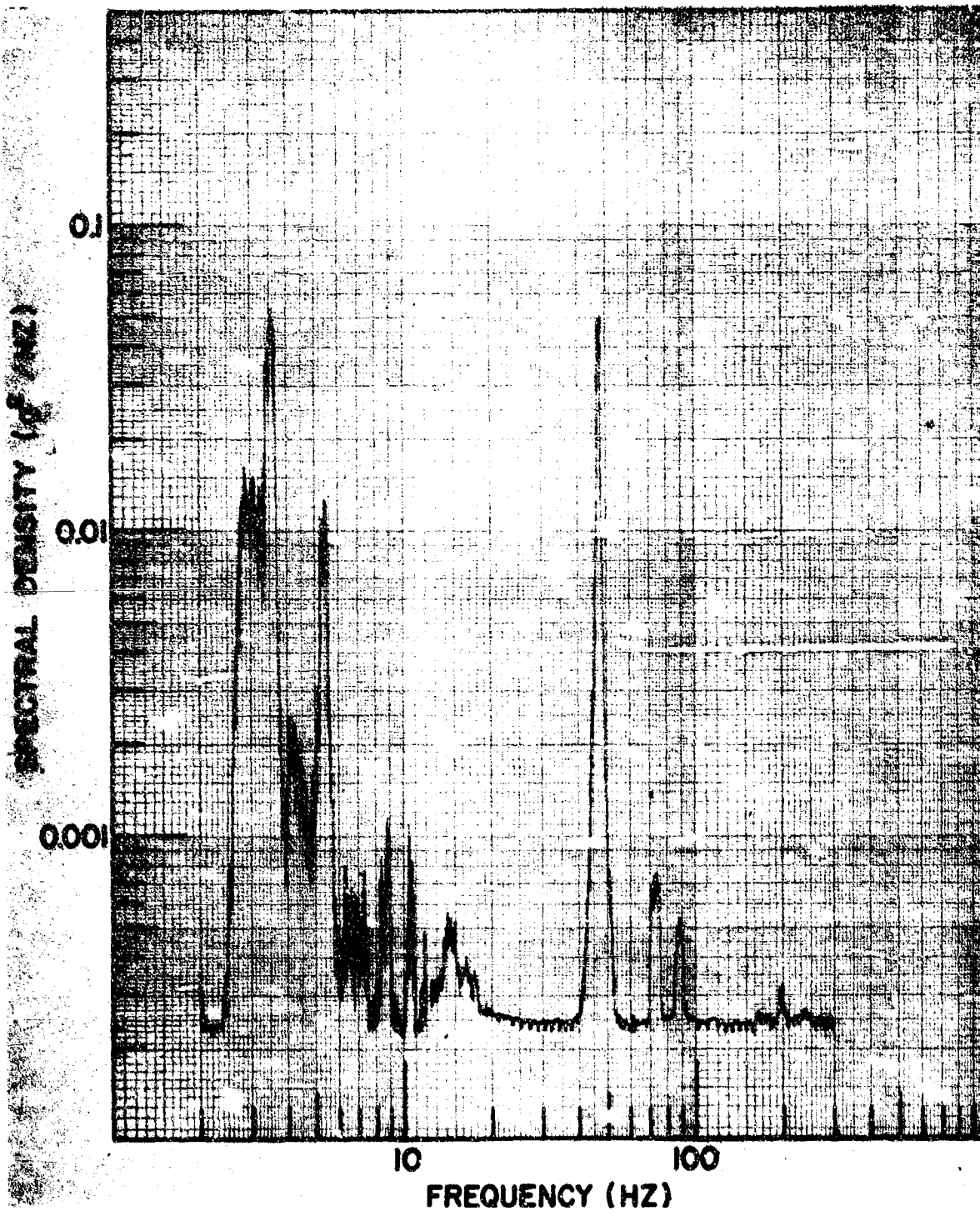
(d)

Fig. 7 (cont'd) - Vertical component spectral densities at the various measurement locations at an equivalent speed of 5 m/h with zero load. Effective analysis filter bandwidths are: 0.25 Hz, 2-12.5 Hz; 1.25 Hz, 12.5-62.5 Hz; 6.25 Hz, 62.5-300 Hz. A: Loc. 11, B: Loc. 12, C: Loc. 13, D: Loc. 21, E: Loc. 22, F: Loc. 23, G: Loc. 31, H: Loc. 32, I: Loc. 33, J: Loc. 41, K: Loc. 42, L: Loc. 43.



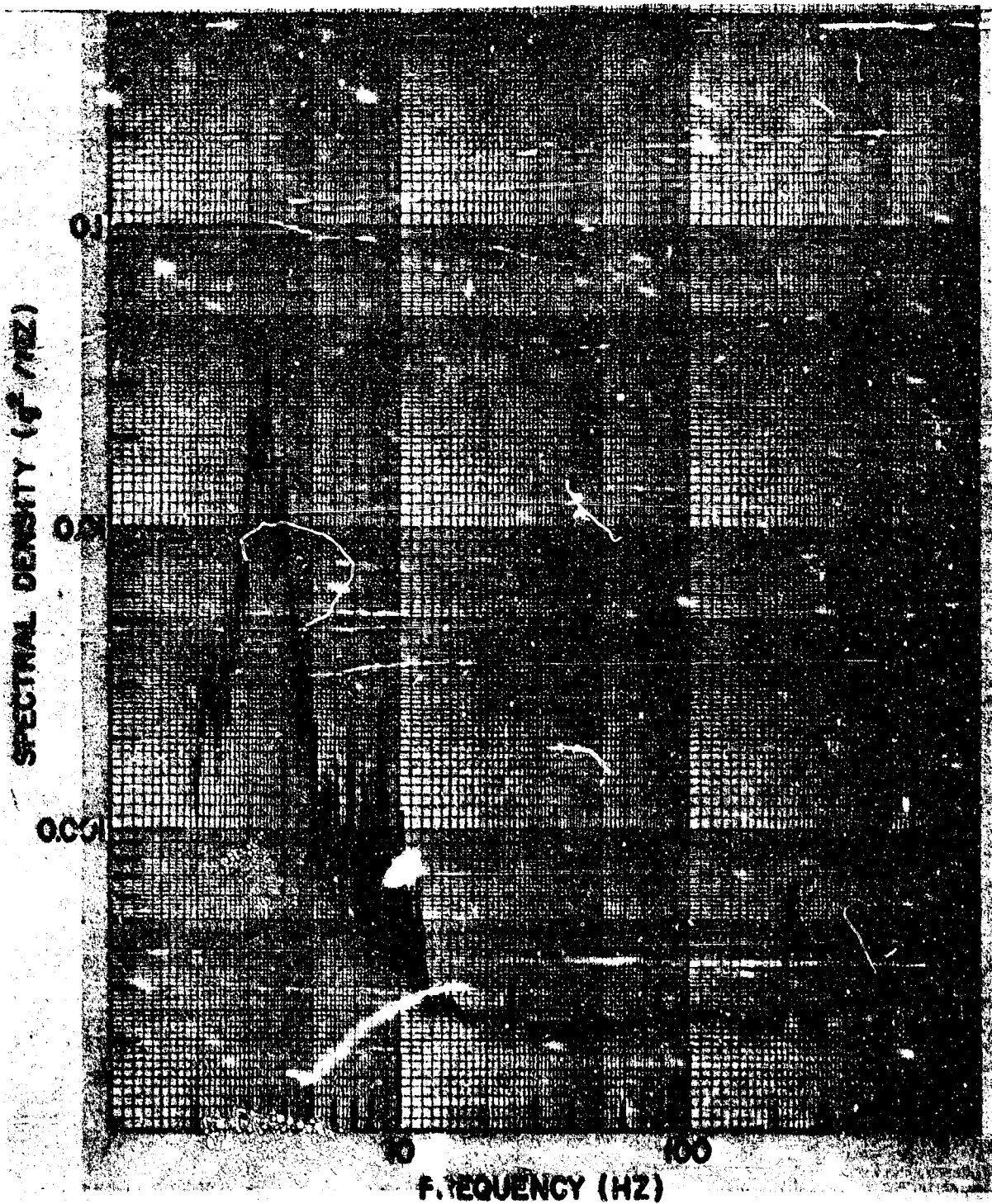
(e)

Fig. 7 (cont'd) - Vertical component spectral densities at the various measurement locations at an equivalent speed of 5 m/h with zero load. Effective analysis filter bandwidths are: 0.25 Hz, 2-12.5 Hz; 1.25 Hz, 12.5-62.5 Hz; 6.25 Hz, 62.5-300 Hz. A: Loc. 11, B: Loc. 12, C: Loc. 13, D: Loc. 21, E: Loc. 22, F: Loc. 23, G: Loc. 31, H: Loc. 32, I: Loc. 33, J: Loc. 41, K: Loc. 42, L: Loc. 43.



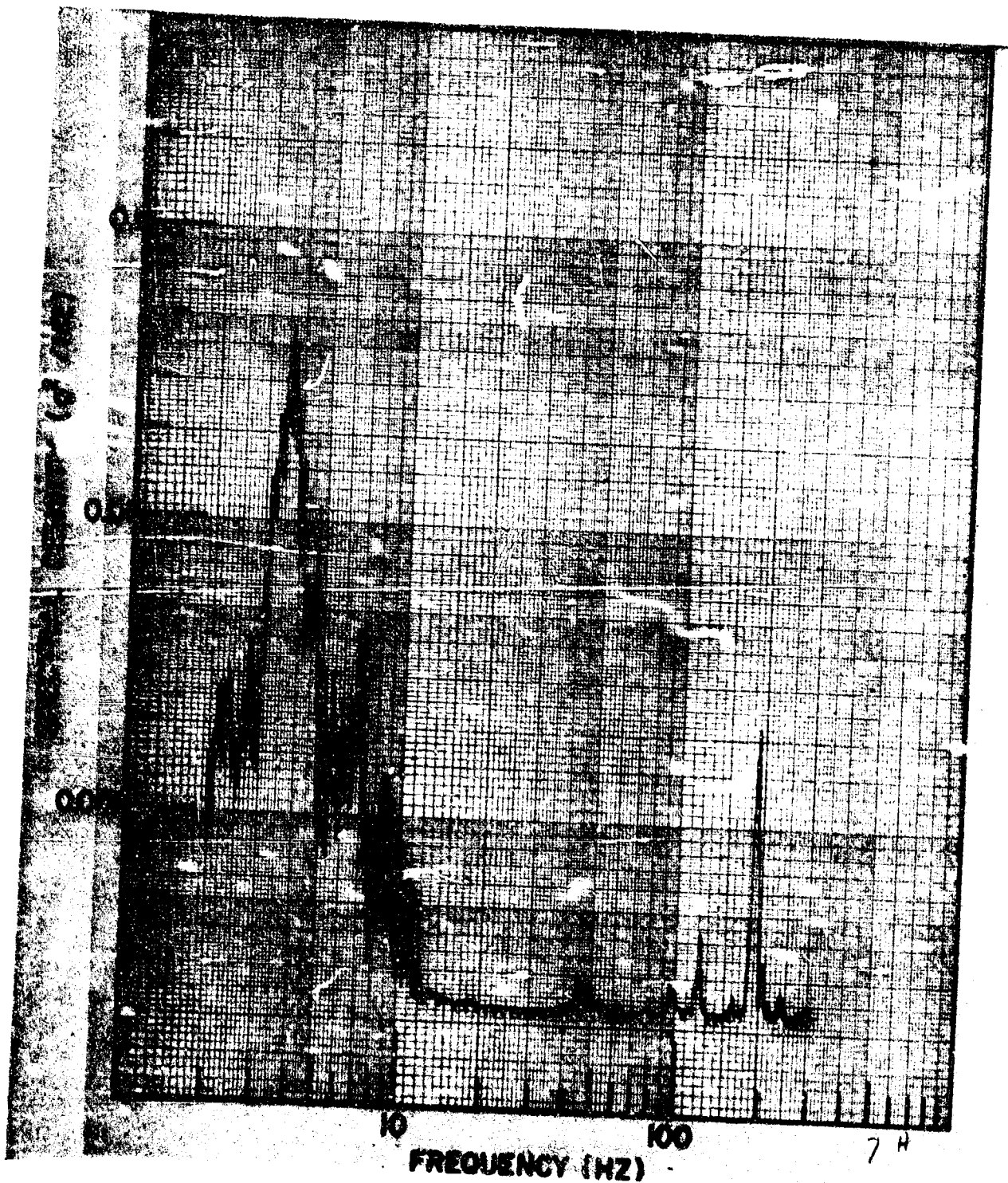
(f)

Fig. 7 (cont'd) - Vertical component spectral densities at the various measurement locations at an equivalent speed of 5 m/h with zero load. Effective analysis filter bandwidths are: 0.25 Hz, 2-12.5 Hz; 1.25 Hz, 12.5-62.5 Hz; 5.25 Hz, 62.5-300 Hz. A: Loc. 11, B: Loc. 12, C: Loc. 13, D: Loc. 21, E: Loc. 22, F: Loc. 23, G: Loc. 31, H: Loc. 32, I: Loc. 33, J: Loc. 41, K: Loc. 42, L: Loc. 43.



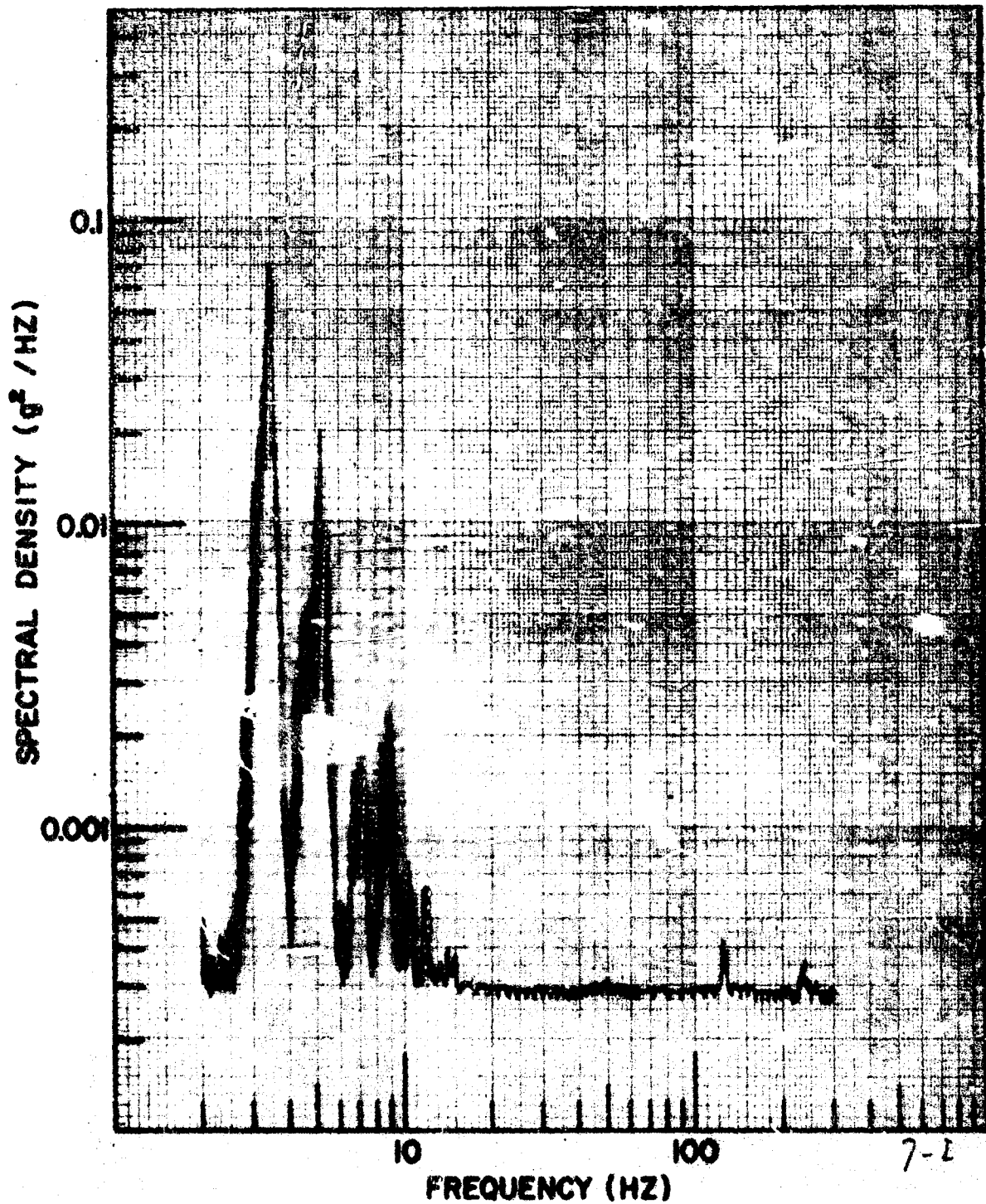
(g)

Fig. 7 (cont'd) - Vertical component spectral densities at the various measurement locations at an equivalent speed of 5 m/h with zero load. Effective analysis filter bandwidths are: 0.25 Hz, 2-12.5 Hz; 1.25 Hz, 12.5-62.5 Hz; 6.25 Hz, 62.5-300 Hz. A: Loc. 11, B: Loc. 12, C: Loc. 13, D: Loc. 21, E: Loc. 22, F: Loc. 23, G: Loc. 31, H: Loc. 32, I: Loc. 33, J: Loc. 41, K: Loc. 42, L: Loc. 43.



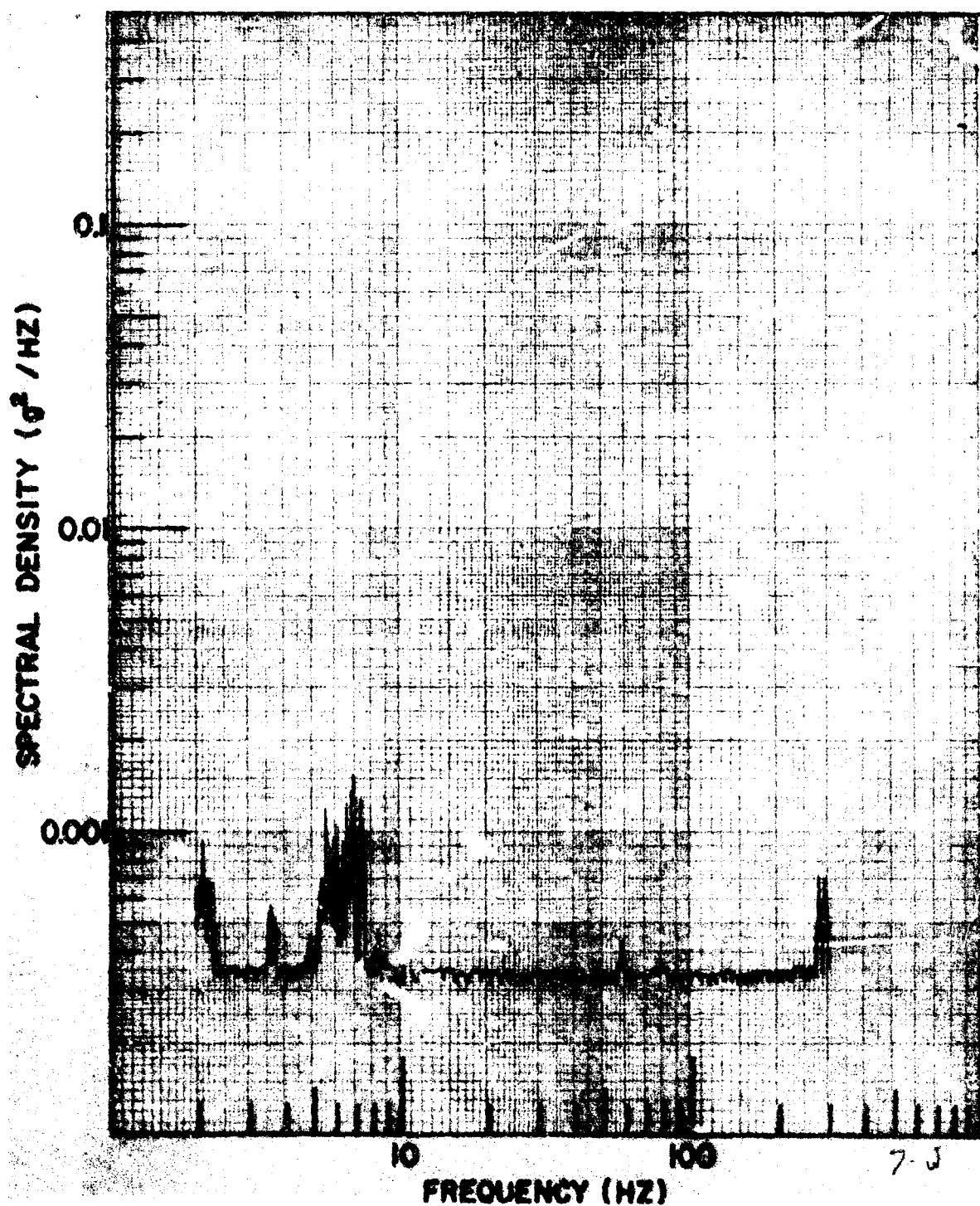
(h)

Fig. 7 (cont'd) - Vertical component spectral densities at the various measurement locations at an equivalent speed of 5 m/h with zero load. Effective analysis filter bandwidths are: 0.25 Hz, 2-12.5 Hz; 1.25 Hz, 12.5-62.5 Hz; 6.25 Hz, 62.5-300 Hz. A: Loc. 11, B: Loc. 12, C: Loc. 13, D: Loc. 21, E: Loc. 22, F: Loc. 23, G: Loc. 31, H: Loc. 32, I: Loc. 33, J: Loc. 41, K: Loc. 42, L: Loc. 43.



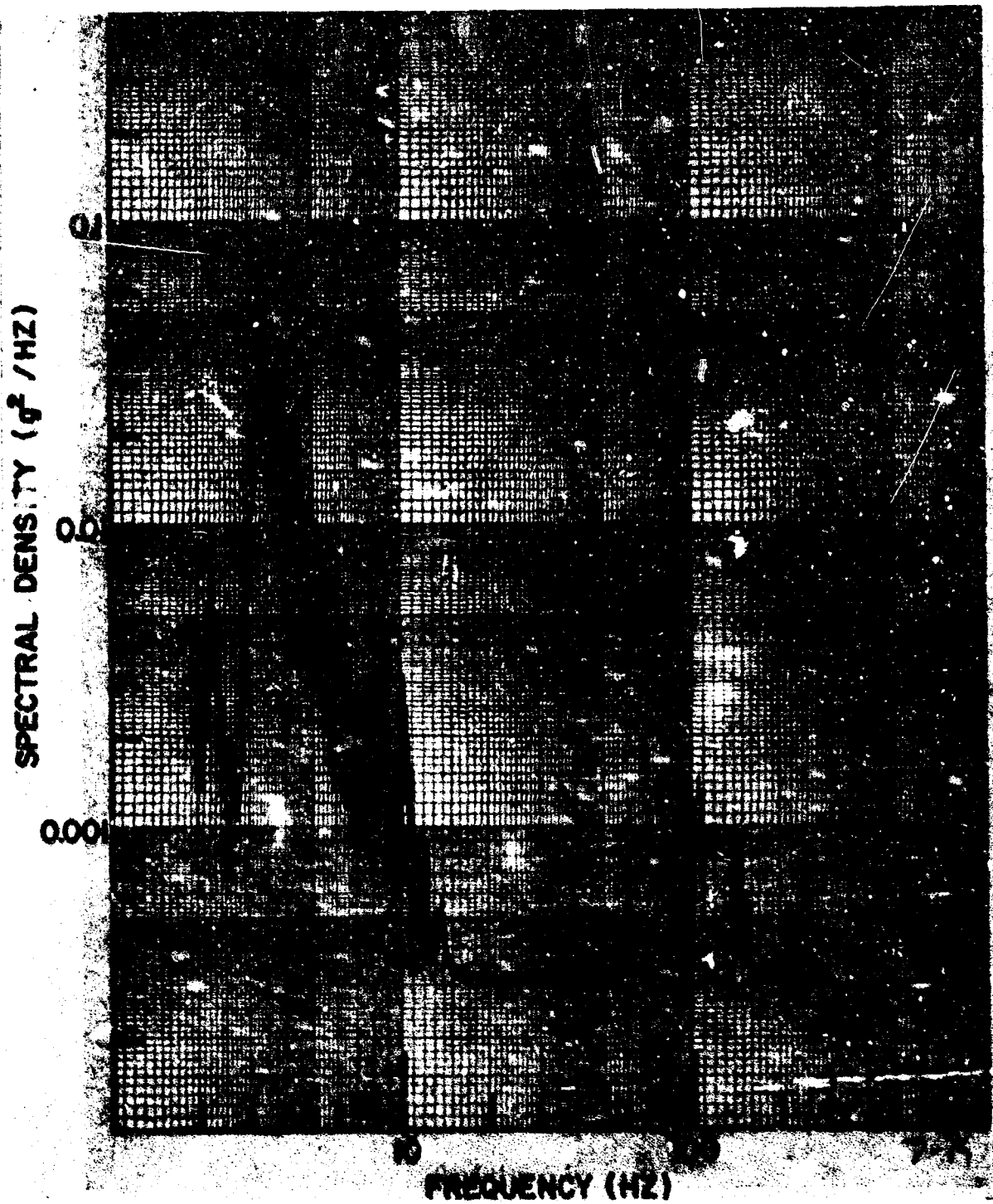
(1)

Fig. 7 (cont'd) - Vertical component spectral densities at the various measurement locations at an equivalent speed of 5 m/h with zero load. Effective analysis filter bandwidths are: 0.25 Hz, 2-12.5 Hz; 1.25 Hz, 12.5-62.5 Hz; 6.25 Hz, 62.5-300 Hz. A: Loc. 11, B: Loc. 12, C: Loc. 13, D: Loc. 21, E: Loc. 22, F: Loc. 23, G: Loc. 31, H: Loc. 32, I: 33, J: Loc. 41, K: Loc. 42, L: Loc. 43.



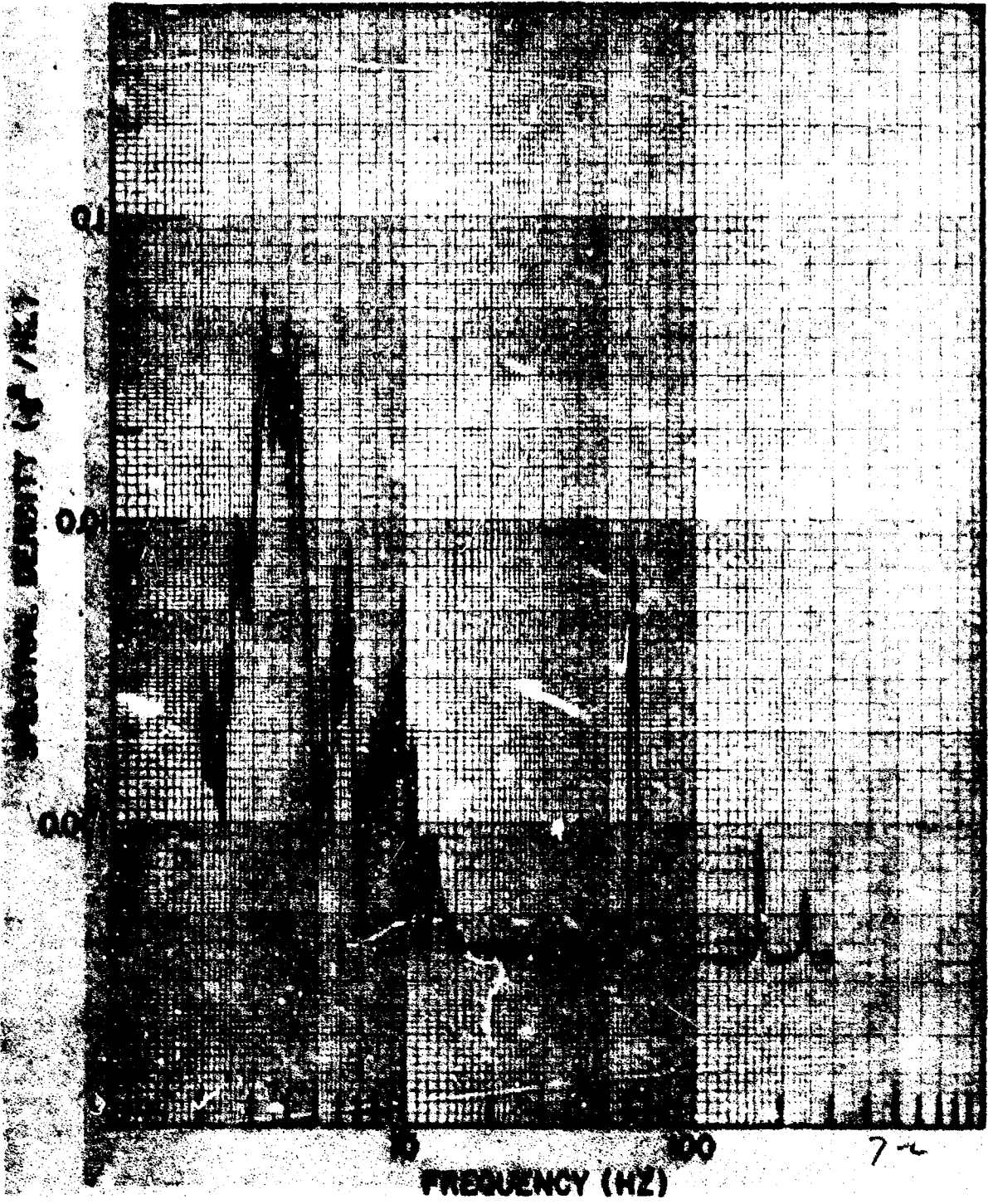
(j)

Fig. 7 (cont'd) - Vertical component spectral densities at the various measurement locations at an equivalent speed of 5 m/h with zero load. Effective analysis filter bandwidths are: 0.25 Hz, 2-12.5 Hz; 1.25 Hz, 12.5-62.5 Hz; 6.25 Hz, 62.5-300 Hz. A: Loc. 11, B: Loc. 12, C: Loc. 13, D: Loc. 21, E: Loc. 22, F: Loc. 23, G: Loc. 31, H: Loc. 32, I: Loc. 33, J: Loc. 41, K: Loc. 42, L: Loc. 43.



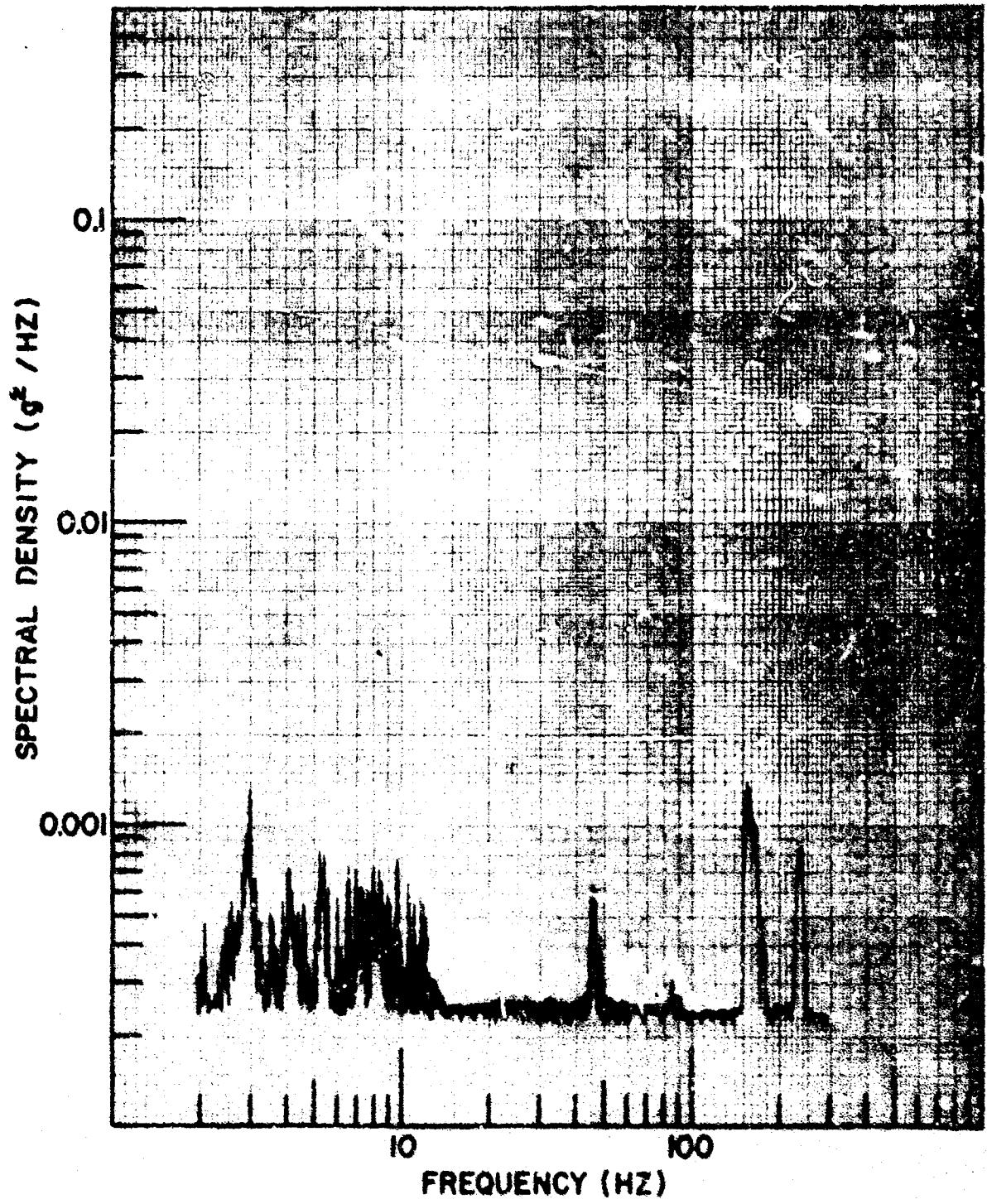
(k)

Fig. 7 (cont'd) - Vertical component spectral densities at the various measurement locations at an equivalent speed of 5 m/h with zero load. Effective analysis filter bandwidths are: 0.25 Hz, 2-12.5 Hz; 1.25 Hz, 12.5-62.5 Hz; 6.25 Hz, 62.5-300 Hz. A: Loc. 11, B: Loc. 12, C: Loc. 13, D: Loc. 21, E: Loc. 22, F: Loc. 23, G: Loc. 31, H: Loc. 32, I: Loc. 33, J: Loc. 41, K: Loc. 42, L: Loc. 43.



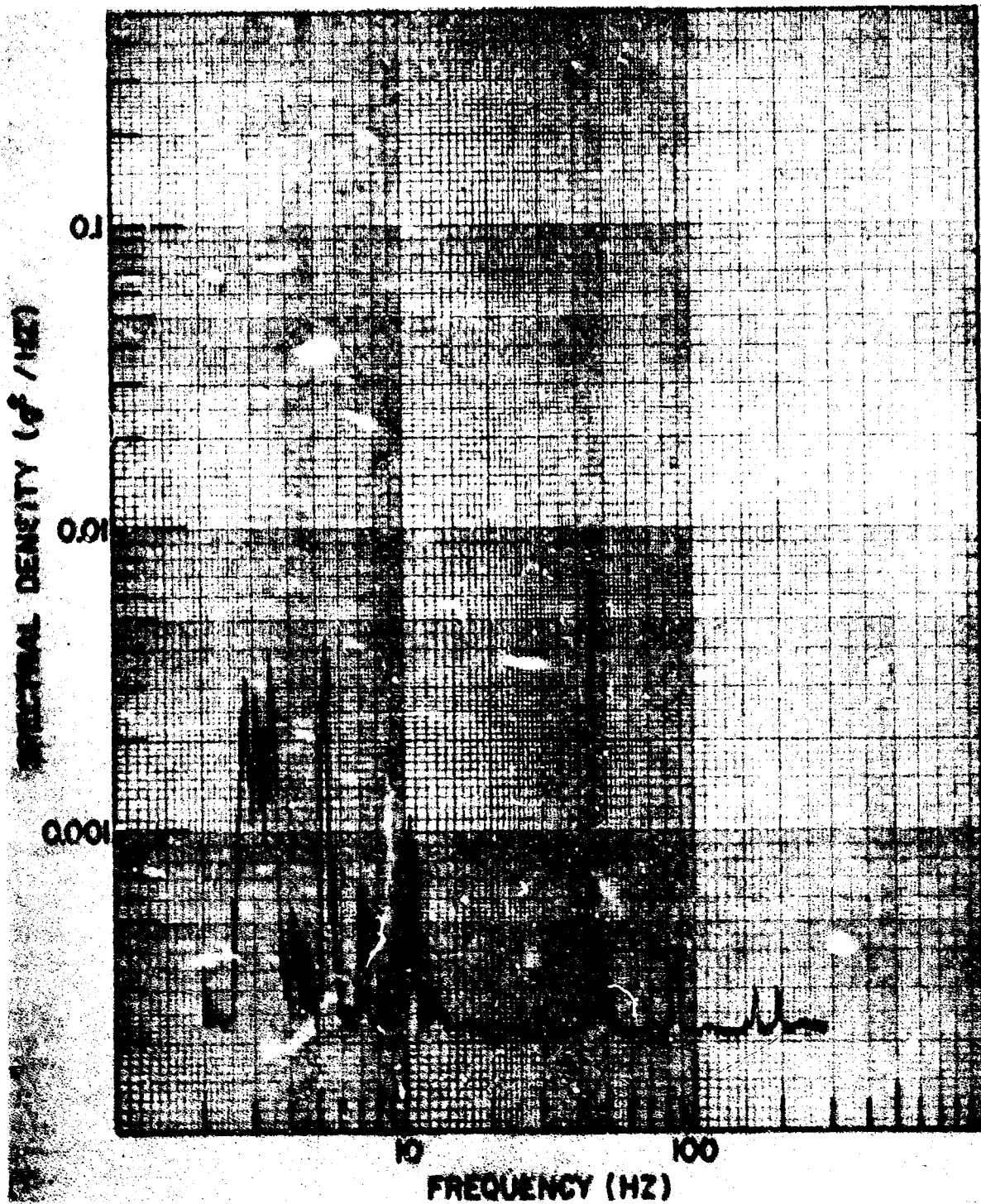
(1)

Fig. 7 (cont'd) - Vertical component spectral densities at the various measurement locations at an equivalent speed of 5 m/h with zero load. Effective analysis filter bandwidths are: 0.25 Hz, 2-12.5 Hz; 1.25 Hz, 12.5-62.5 Hz; 6.25 Hz, 62.5-300 Hz. A: Loc. 11, B: Loc. 12, C: Loc. 13, D: Loc. 21, E: Loc. 22, F: Loc. 23, G: Loc. 31, H: Loc. 32, I: Loc. 33, J: Loc. 41, K: Loc. 42, L: Loc. 43.



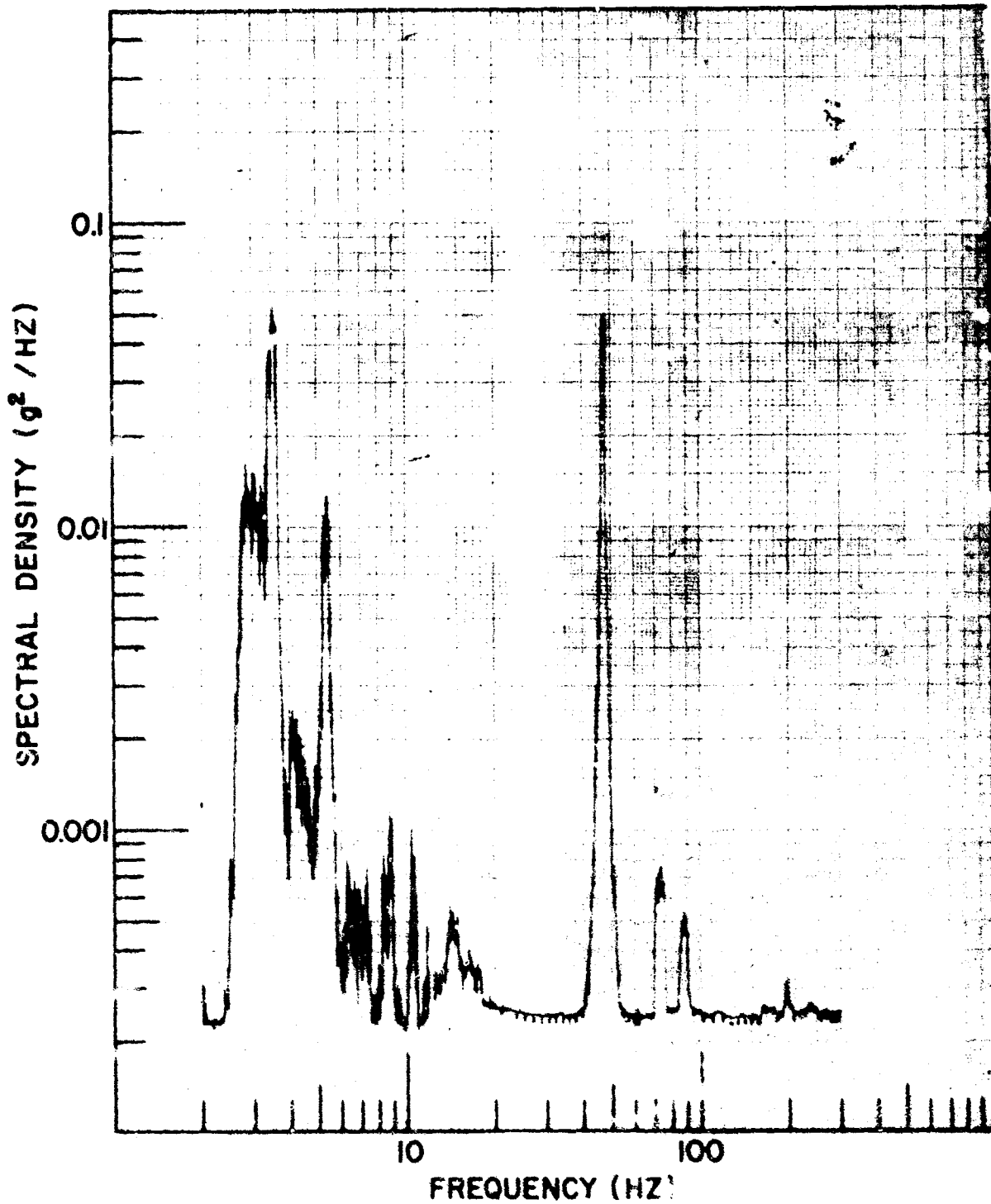
(a)

Fig. 8 - Spectral densities of component accelerations at location 23 for speeds of 5, 10 and 20 m/h with zero load. Effective analysis filter bandwidths are: 0.25 Hz, 2-12 .5 Hz; 1.25 Hz, 12.5-62.5 Hz; 6.25 Hz, 62.5-300 Hz. A: Longitudinal, 5 m/h; B: Transverse, 5 m/h; C: Vertical, 5 m/h; D: Longitudinal, 10 m/h; E: Transverse, 10 m/h; F: Vertical, 10 m/h; G: Longitudinal, 20 m/h; H: Transverse, 20 m/h; I: Vertical, 20 m/h.



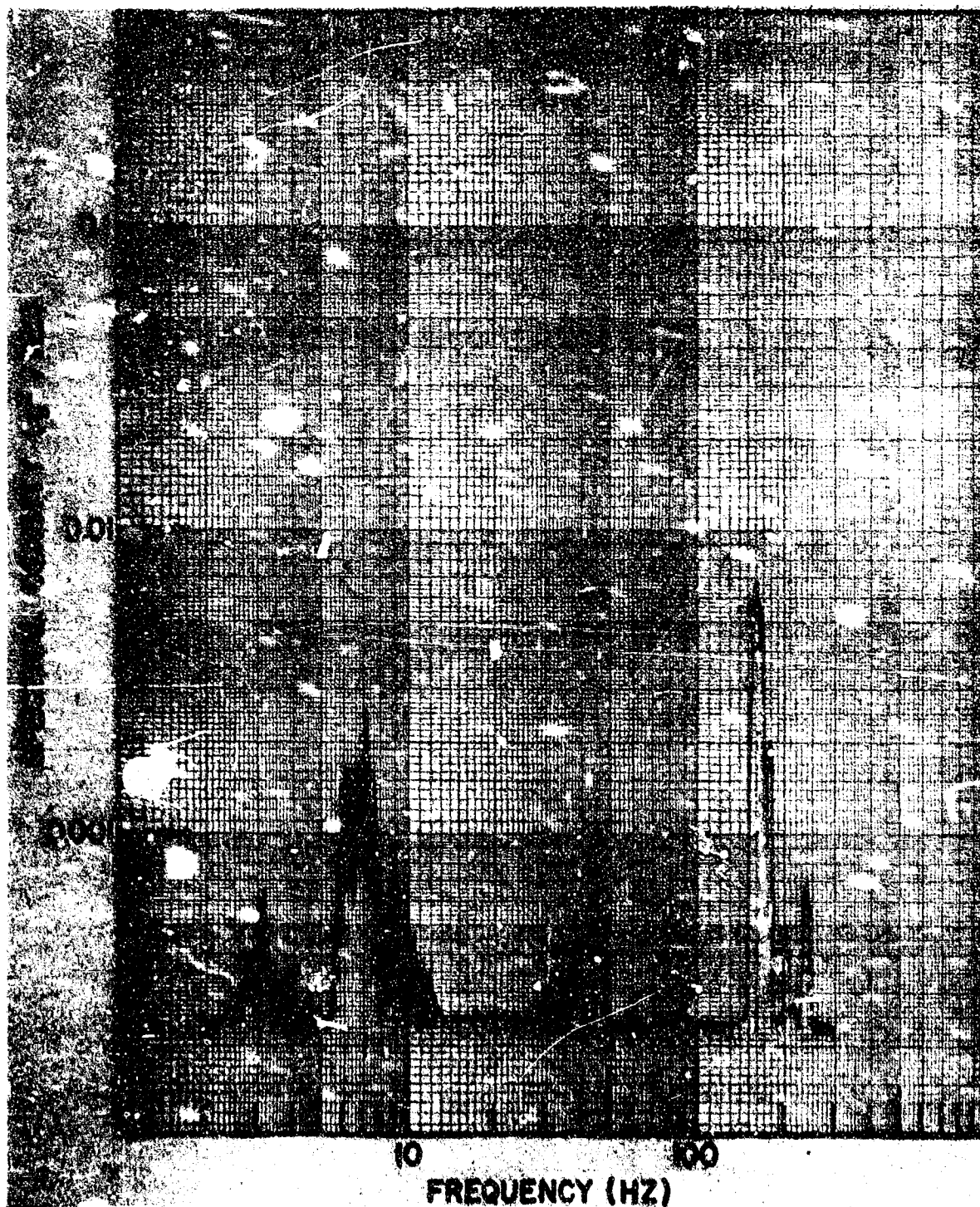
(b)

Fig. 8 (cont'd) - Spectral densities of component accelerations at location 23 for speeds of 5, 10 and 20 m/h with zero load. Effective analysis filter bandwidths are: 0.25 Hz, 2-12.5 Hz; 1.25 Hz, 12.5-62.5 Hz; 6.25 Hz, 62.5-300 Hz. A: Longitudinal, 5 m/h; B: Transverse, 5 m/h; C: Vertical, 5 m/h; D: Longitudinal, 10 m/h; E: Transverse, 10 m/h; F: Vertical, 10 m/h; G: Longitudinal, 20 m/h; H: Transverse, 20 m/h; I: Vertical, 20 m/h.



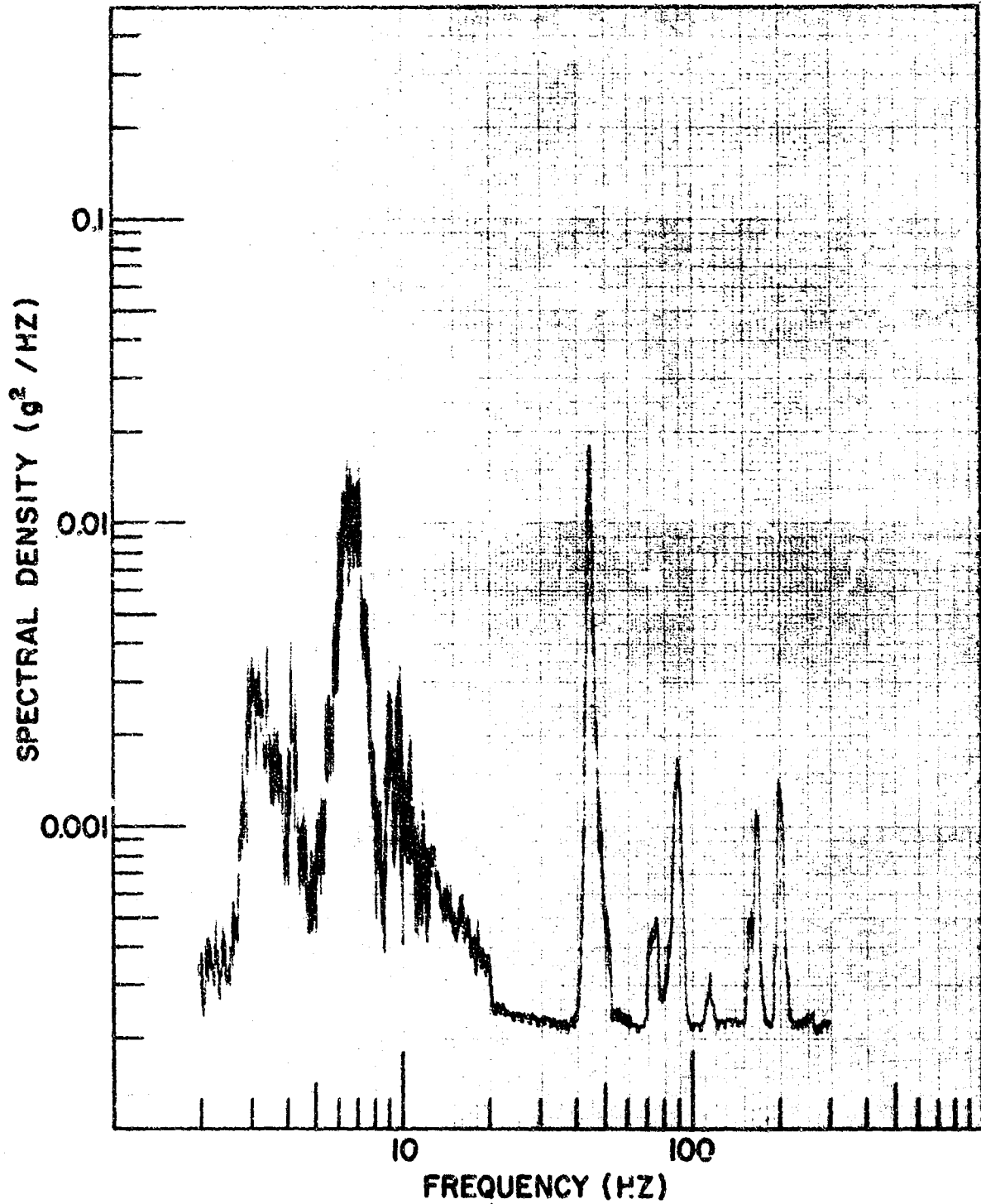
(c)

Fig. 8 (cont'd) - Spectral densities of component accelerations at location 23 for speeds of 5, 10 and 20 m/h with zero load. Effective analysis filter bandwidths are: 0.25 Hz, 2-12.5 Hz; 1.25 Hz, 12.5-62.5 Hz; 6.25 Hz, 62.5-300 Hz. AA: Longitudinal, 5 m/h; B: Transverse, 5 m/h; C: Vertical, 5 m/h; D: Longitudinal, 10 m/h; E: Transverse, 10 m/h; F: Vertical, 10 m/h; G: Longitudinal, 20 m/h; H: Transverse, 20 m/h; I: Vertical, 20 m/h.



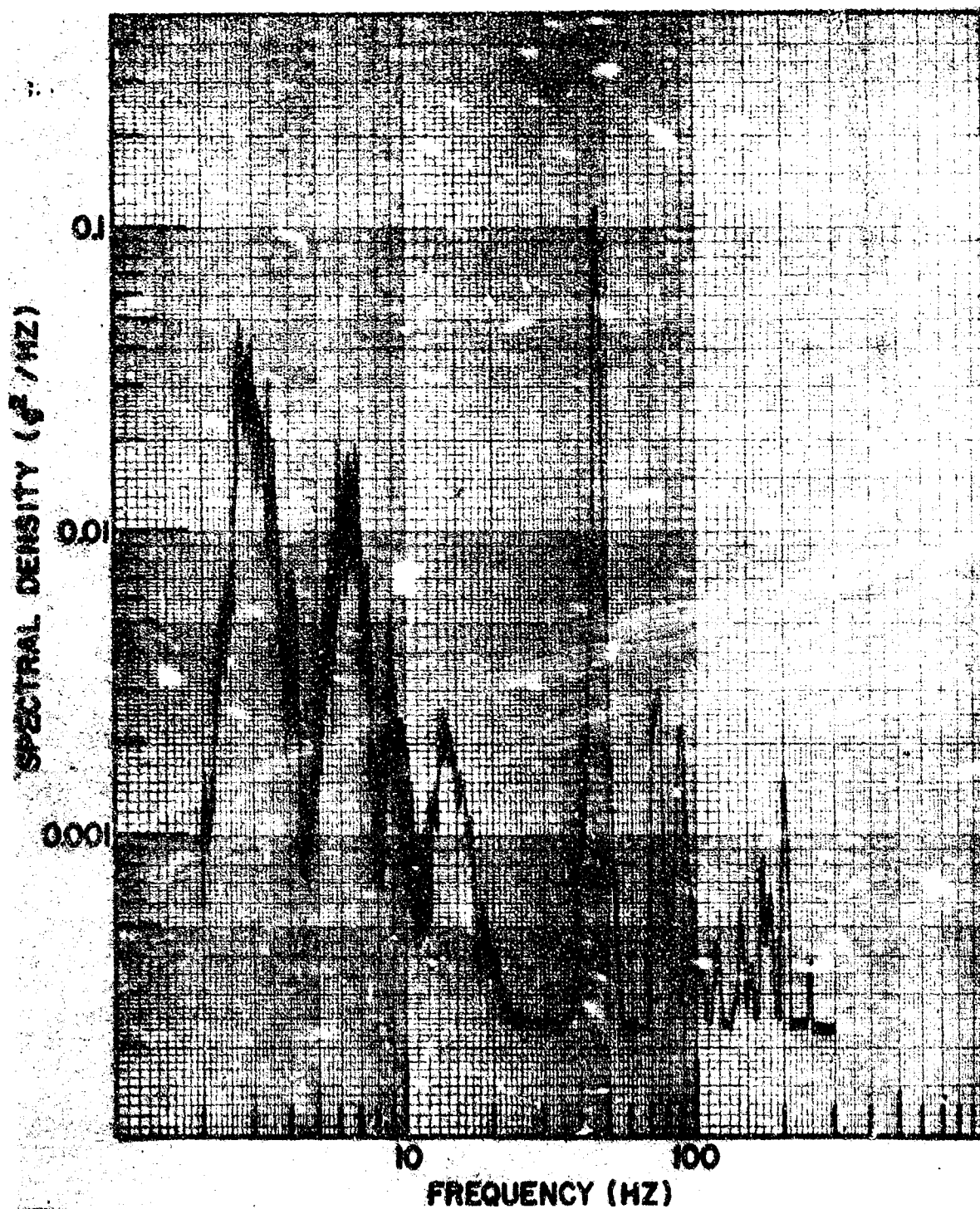
(d)

Fig. 8 (cont'd) - Spectral densities of component accelerations at location 23 for speeds of 5, 10 and 20 m/h with zero load. Effective analysis filter bandwidths are: 0.25 Hz, 2-12.5 Hz; 1.25 Hz, 12.5-62.5 Hz; 6.25 Hz, 62.5-300 Hz. A: Longitudinal, 5 m/h; B: Transverse, 5 m/h; C: Vertical, 5 m/h; D: Longitudinal, 10 m/h; E: Transverse, 10 m/h; F: Vertical, 10 m/h; G: Longitudinal, 20 m/h; H: Transverse, 20 m/h; I: Vertical, 20 m/h.



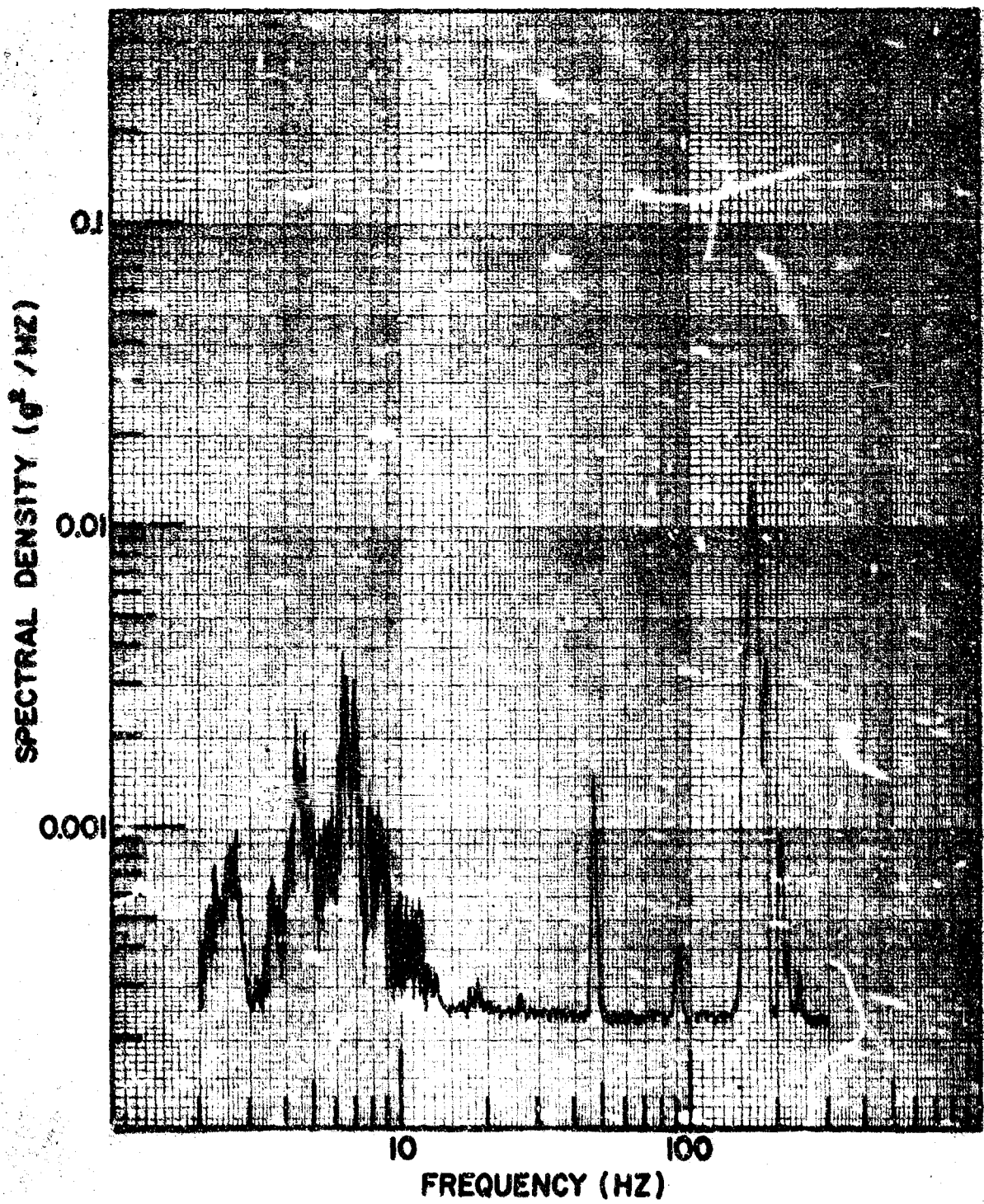
(e)

Fig. 8 (cont'd) - Spectral densities of component accelerations at location 23 for speeds of 5, 10 and 20 m/h with zero load. Effective analysis filter bandwidths are: 0.25 Hz, 2-12.5 Hz; 1.25 Hz, 12.5-62.5 Hz; 6.25 Hz, 62.5-300 Hz. A: Longitudinal, 5 m/h; B: Transverse, 5 m/h; C: Vertical, 5 m/h; D: Longitudinal, 10 m/h; E: Transverse, 10 m/h; F: Vertical, 10 m/h; G: Longitudinal, 20 m/h; H: Transverse, 20 m/h; I: Vertical, 20 m/h.



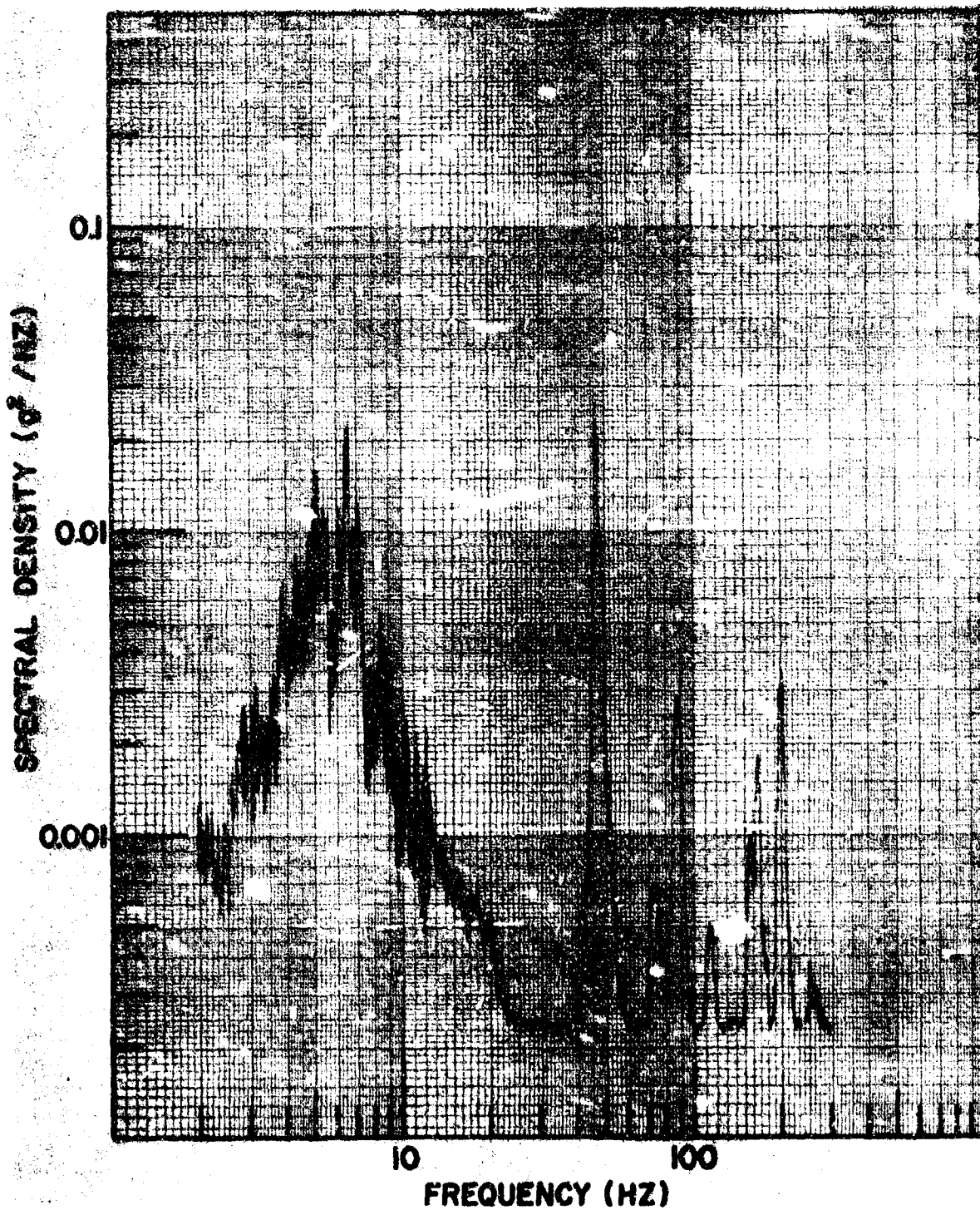
(f)

Fig. 8 (cont'd) - Spectral densities of component accelerations at location 23 for speeds of 5, 10 and 20 m/h with zero load. Effective analysis filter bandwidths are: 0.25 Hz, 2-12.5 Hz; 1.25 Hz, 12.5-62.5 Hz; 6.25 Hz, 62.5-300 Hz. A: Longitudinal, 5 m/h; B: Transverse, 5 m/h; C: Vertical, 5 m/h; D: Longitudinal, 10 m/h; E: Transverse, 10 m/h, F: Vertical, 10 m/h; G: Longitudinal, 20 m/h; H: Transverse, 20 m/h; I: Vertical, 20 m/h.



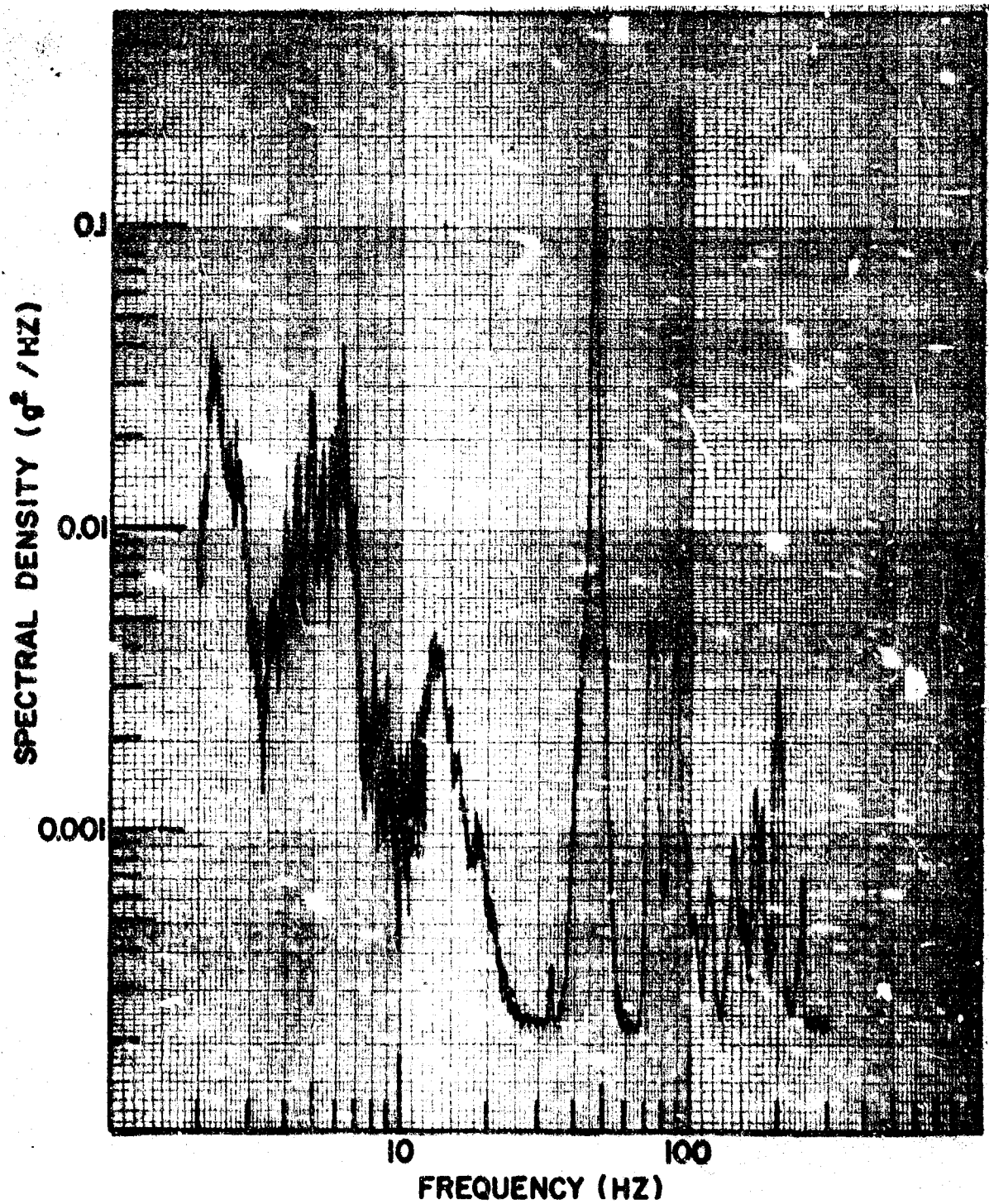
(g)

Fig. 8 (cont'd) - Spectral densities of component accelerations at location 23 for speeds of 5, 10 and 20 m/h with zero load. Effective analysis filter bandwidths are: 0.25 Hz, 2-12.5 Hz; 1.25 Hz, 12.5-62.5 Hz; 6.25 Hz, 62.5-300 Hz. A: Longitudinal, 5 m/h; B: Transverse, 5 m/h; C: Vertical, 5 m/h; D: Longitudinal, 10 m/h; E: Transverse, 10 m/h; F: Vertical, 10 m/h; G: Longitudinal, 20 m/h; H: Transverse, 20 m/h; I: Vertical, 20 m/h.



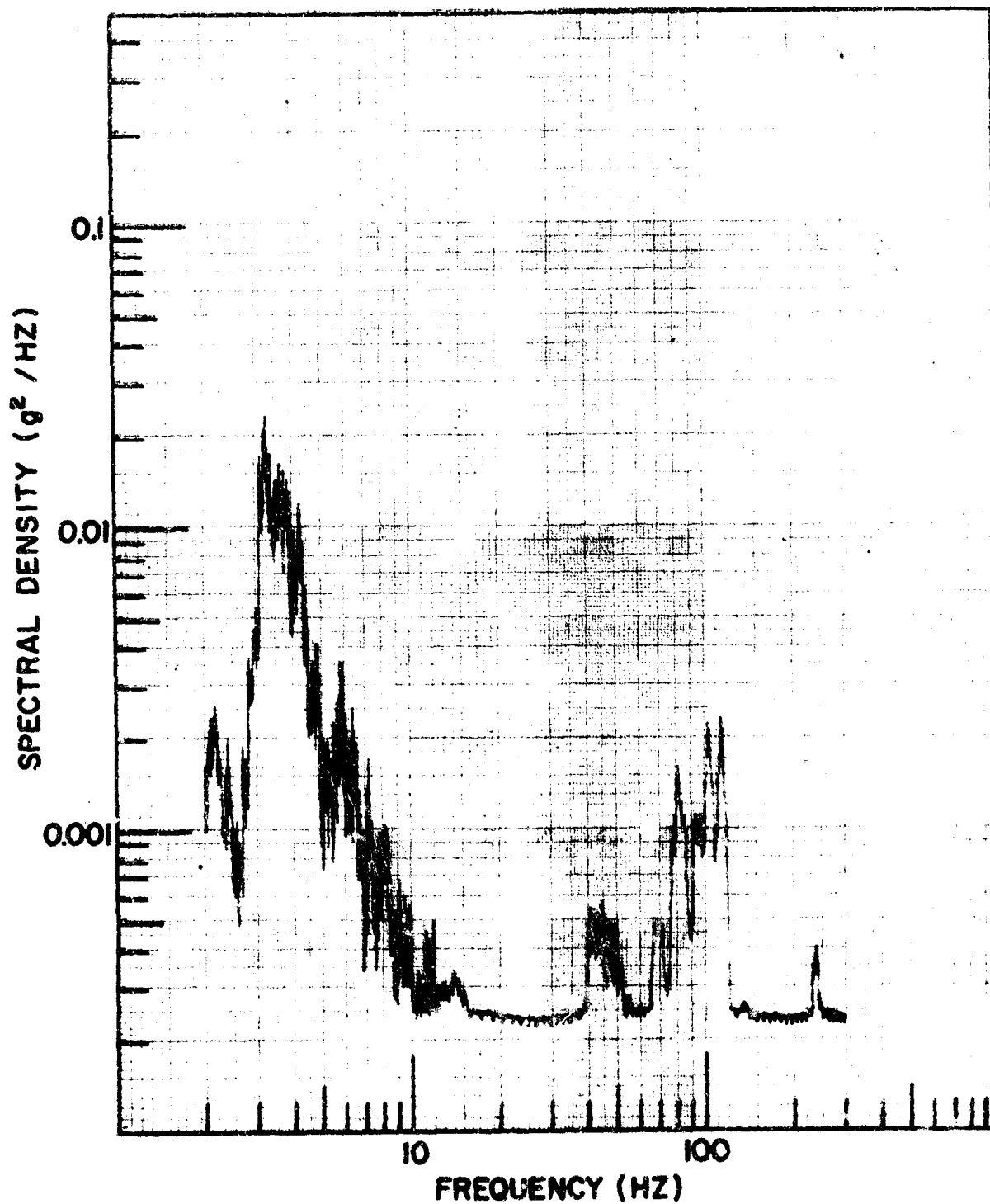
(h)

Fig. 8 (cont'd) - Spectral densities of component accelerations at location 23 for speeds of 5, 10 and 20 m/h with zero load. Effective analysis filter bandwidths are: 0.25 Hz, 2-12.5 Hz; 1.25 Hz, 12.5-62.5 Hz; 6.25 Hz, 62.5-300 Hz. A: Longitudinal, 5 m/h; B: Transverse, 5 m/h, C: Vertical, 5 m/h; D: Longitudinal, 10 m/h; E: Transverse, 10 m/h, F: Vertical, 10 m/h; G: Longitudinal, 20 m/h; H: Transverse, 20 m/h; I: Vertical, 20 m/h.



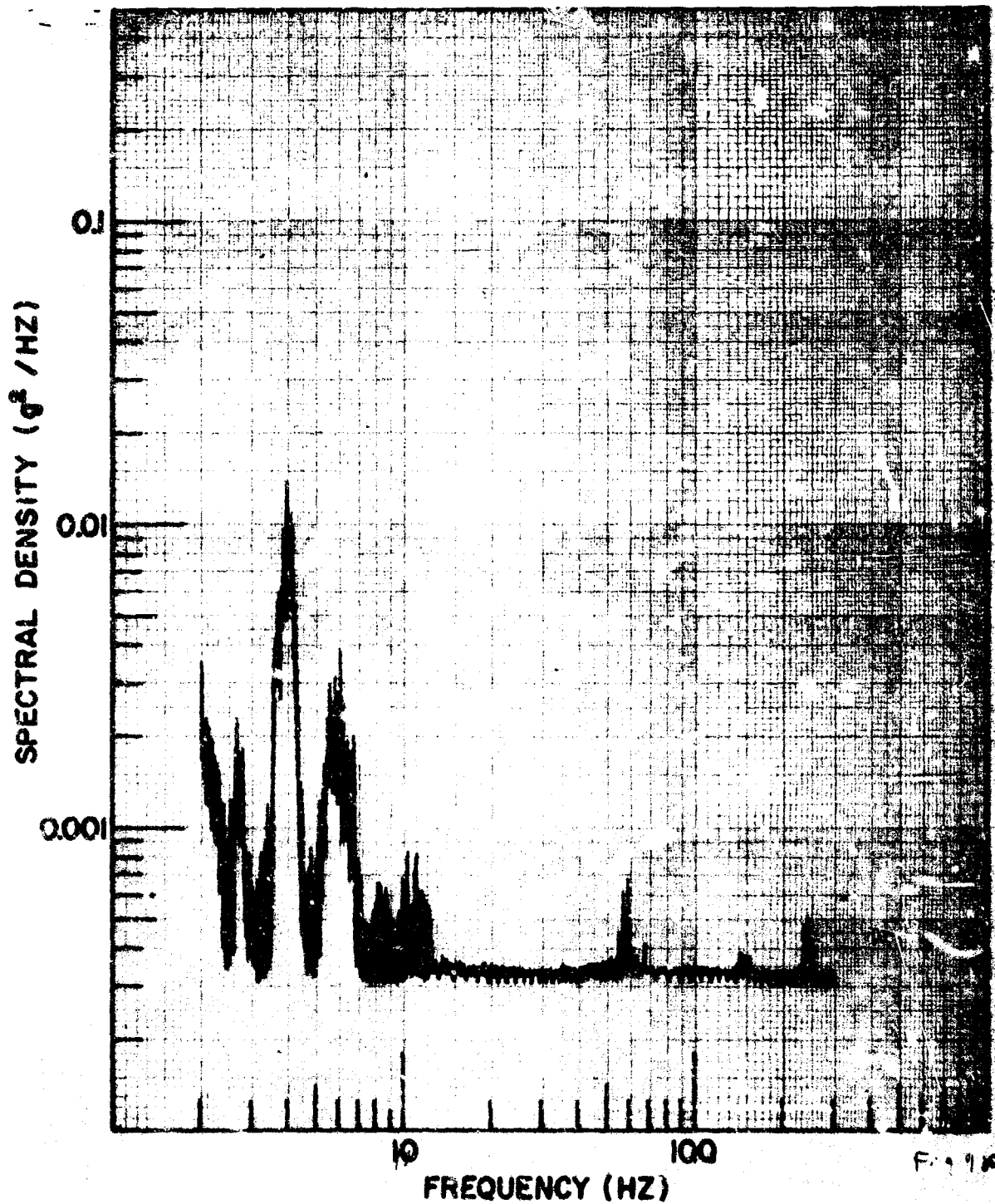
(i)

Fig. 8 (cont'd) -- Spectral densities of component accelerations at location 23 for speeds of 5, 10 and 20 m/h with zero load. Effective analysis filter bandwidths are: 0.25 Hz, 2-12.5 Hz; 1.25 Hz, 12.5-62.5 Hz; 6.25 Hz, 62.5-300 Hz. A: Longitudinal, 5 m/h; B: Transverse, 5 m/h; C: Vertical, 5 m/h; D: Longitudinal, 10 m/h; E: Transverse, 10 m/h; F: Vertical, 10 m/h; G: Longitudinal, 20 m/h; H: Transverse, 20 m/h; I: Vertical, 20 m/h.



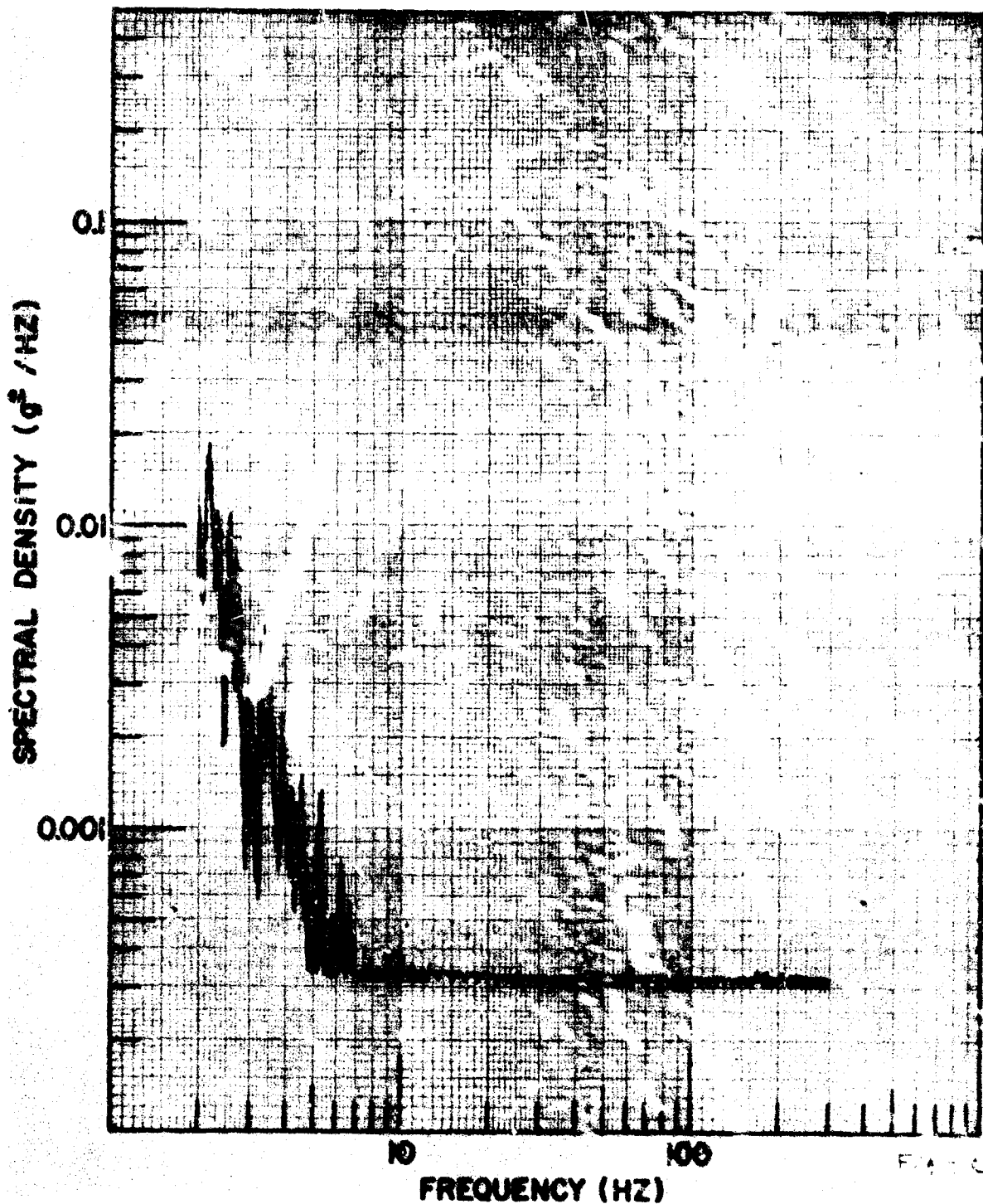
(a)

Fig. 9 - Vertical component spectral densities in the vicinity of the load at speeds of 5 and 20 m/h with zero load, half load and full load. Effective analysis filter bandwidths are: 0.25 Hz, 2-12.5 Hz; 1.25 Hz, 12.5-62.5 Hz; 6.25 Hz, 62.5-300 Hz. A: Loc. 22, zero load, 5 m/h; B: Loc. LL, half load, 5 m/h; C: Loc. L, full load, 5 m/h; D: Loc. 22, zero load, 20 m/h; E: Loc. LL, half load, 20 m/h; F: Loc. L, full load, 20 m/h.



(b)

Fig. 9 (cont'd) - Vertical component spectral densities in the vicinity of the load at speeds of 5 and 20 m/h with zero load, half load and full load. Effective analysis filter bandwidths are: 0.25 Hz, 2-12.5 Hz; 1.25 Hz, 12.5-62.5 Hz; 6.25 Hz, 62.5-300 Hz. A: Loc. 22, zero load, 5 m/h; B: Loc. LL, half load, 5 m/h; C: Loc. L, full load, 5 m/h; D: Loc. 22, zero load, 20 m/h; E: Loc. LL, half load, 20 m/h; F: Loc. L, full load, 20 m/h.



(c)

Fig. 9 (cont'd) - Vertical components spectral densities in the vicinity of the load at speeds of 5 and 20 m/h with zero load, half load and full load. Effective analysis filter bandwidths are: 0.25 Hz, 2-12.5 Hz; 1.25 Hz, 12.5-62.5 Hz; 6.25 Hz, 62.5-390 Hz. A: Loc. 22, zero load, 5 m/h; B: Loc. LL, half load, 5 m/h; C: Loc. L, full load, 5 m/h; D: Loc. 22, zero load, 20 m/h; E: Loc. LL, half load, 20 m/h; F: Loc. L, full load, 20 m/h.

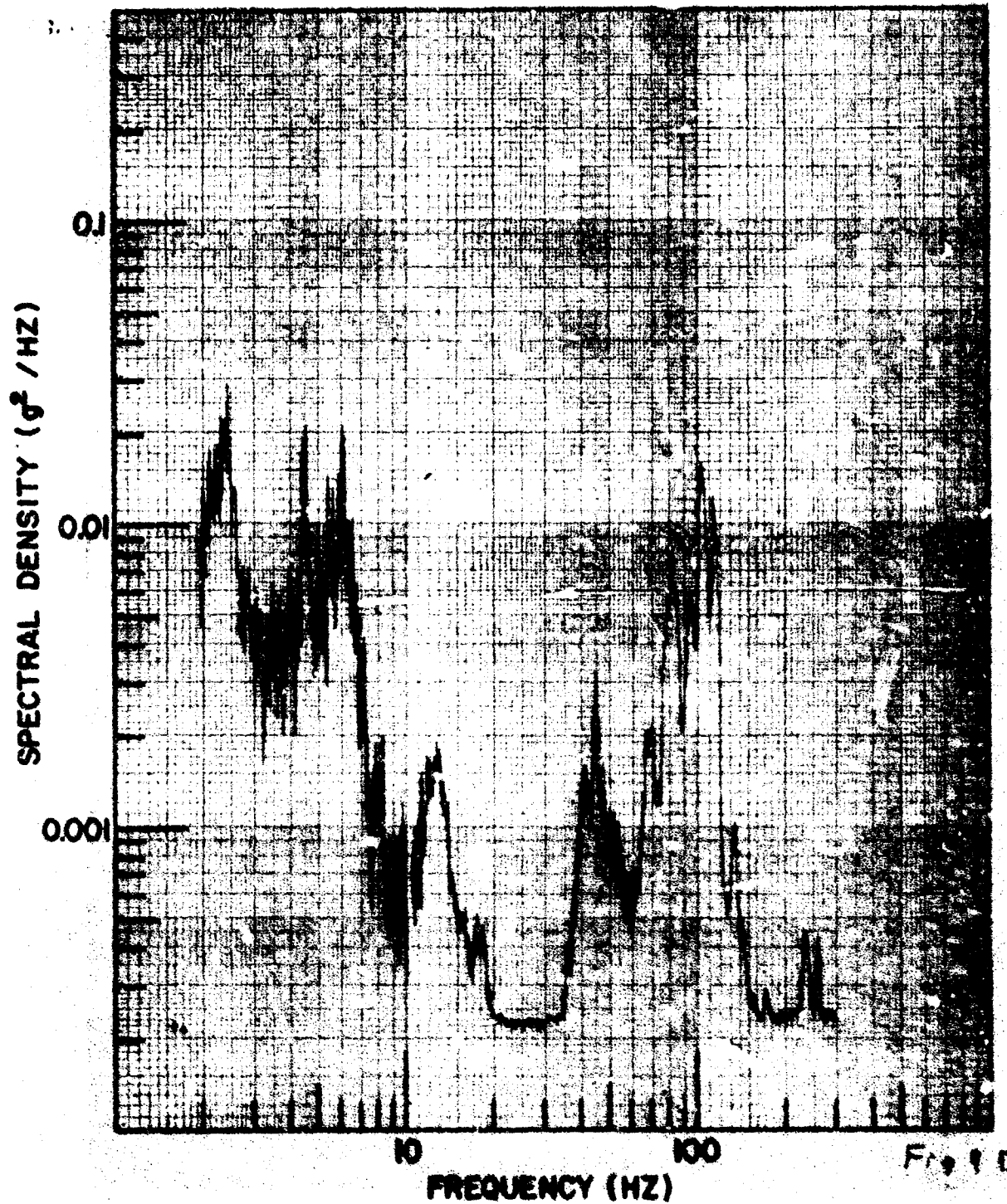
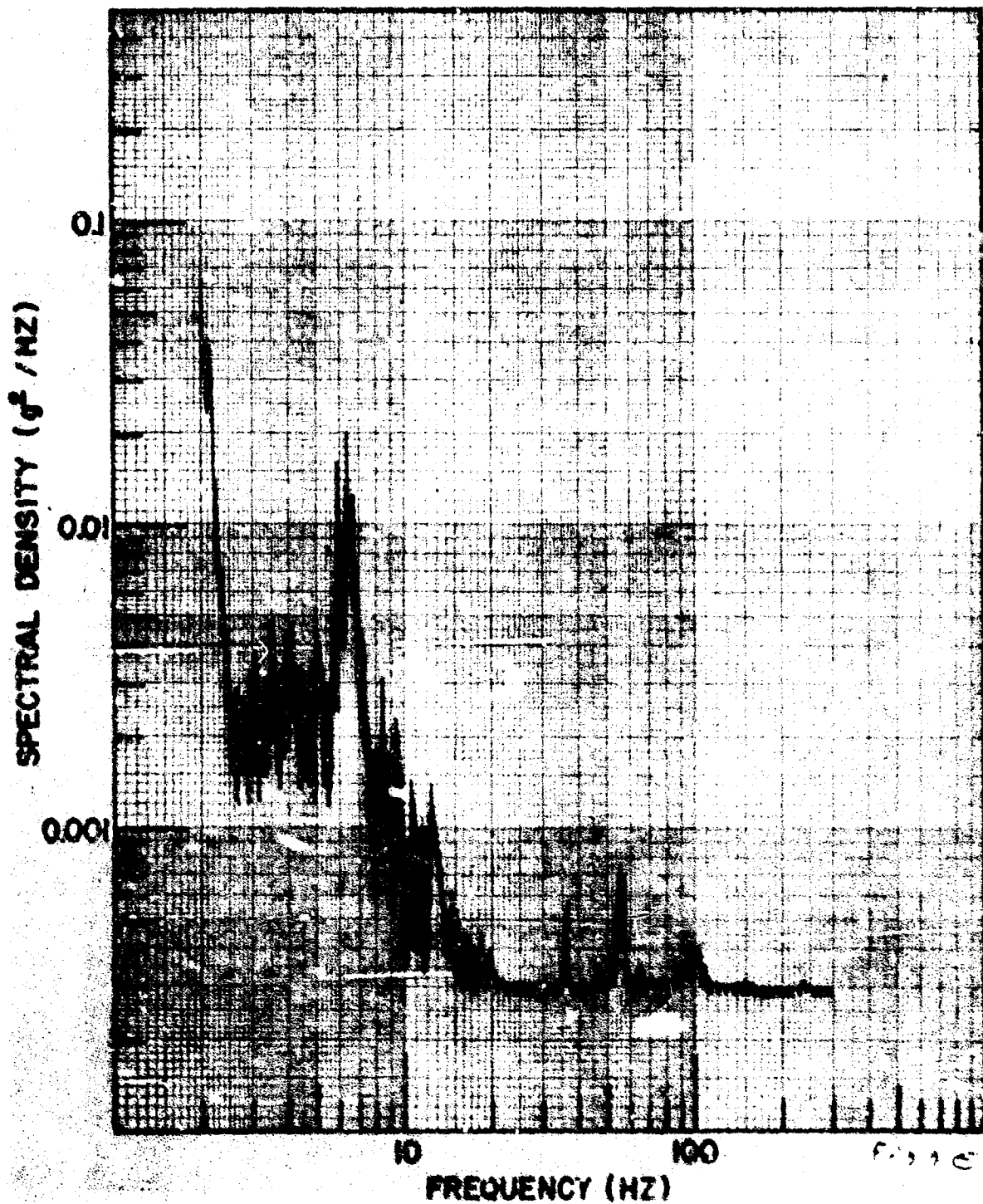
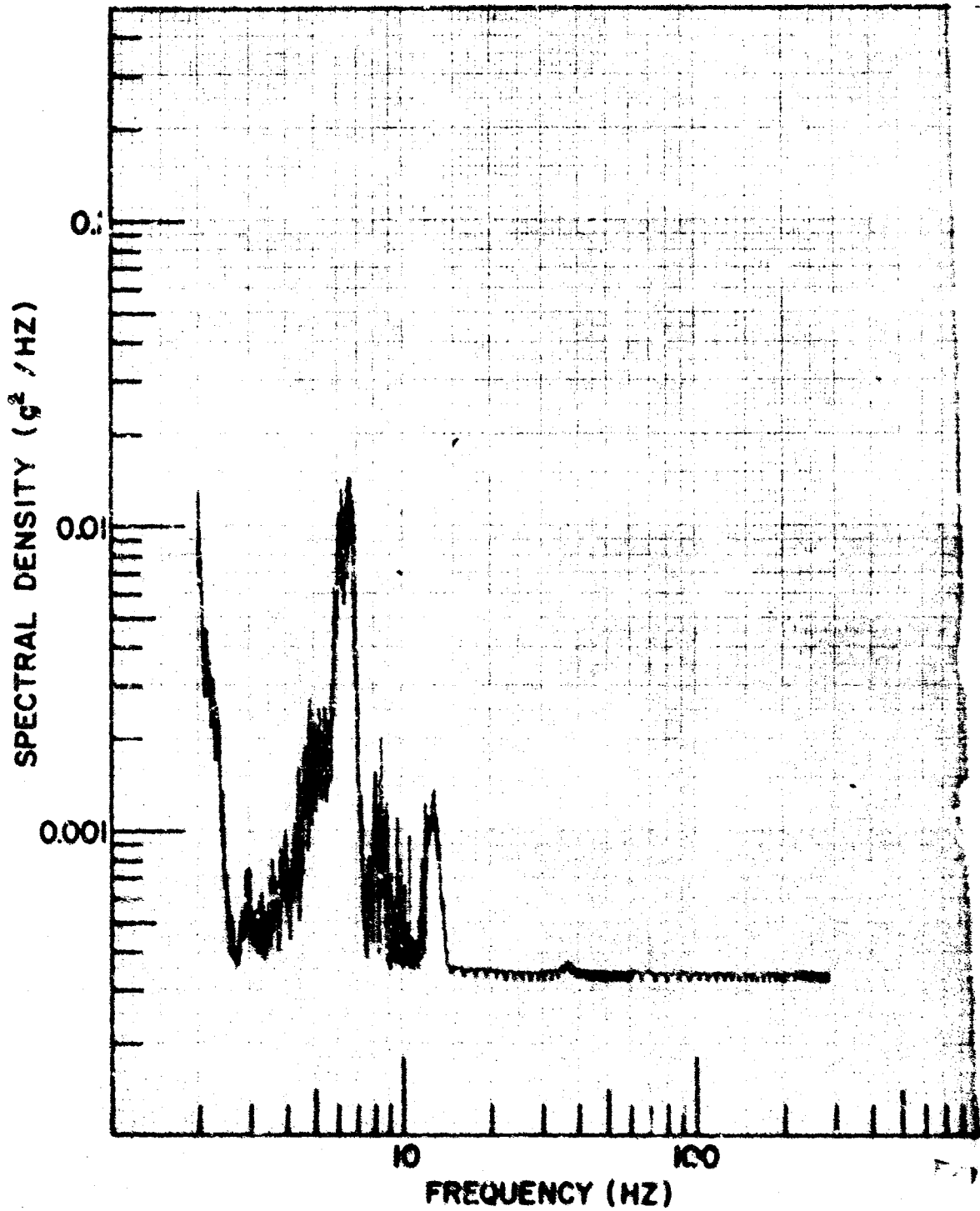


Fig. 9 (cont'd) - Vertical components spectral densities in the vicinity of the load at speeds of 5 and 20 m/h with zero load, half load and full load. Effective analysis filter bandwidths are: 0.25 Hz, 2-12.5 Hz; 1.25 Hz, 12.5-62.5 Hz; 6.25 Hz, 62.5-300 Hz. A: Loc. 22, zero load, 5 m/h; B: Loc. LL, half load, 5 m/h; C: Loc. L, full load, 5 m/h; D: Loc. 22, zero load, 20 m/h; E: Loc. LL, half load, 20 m/h; F: Loc. L, full load, 20 m/h.



(e)

Fig. 9 (cont'd) - Vertical components spectral densities in the vicinity of the load at speeds of 5 and 20 m/h with zero load, half load and full load. Effective analysis filter bandwidths are: 0.25 Hz, 2-12.5 Hz; 1.25 Hz, 12.5-62.5 Hz; 6.25 Hz, 62.5-300 Hz. A: Loc. 22, zero load, 5 m/h; B: Loc. LL, half load, 5 m/h; C: Loc. L, full load, 5 m/h; D: Loc. 22, zero load, 20 m/h; E: Loc. LL, half load, 20 m/h; F: Loc. L, full load, 20 m/h.



(f)

Fig. 9 (cont'd) - Vertical components spectral densities in the vicinity of the load speeds of 5 and 20 m/h with zero load, half load, and full load. Effective analysis filter bandwidths are: 0.25 Hz, 2-12.5 Hz; 1.25 Hz, 12.5-62.5 Hz; 6.25 Hz, 62.5-300 Hz. Loc. 22, zero load, 5 m/h; B: Loc. LL, half load, 5 m/h; C: Loc. L, full load, 5 m/h; Loc. 22, zero load, 20 m/h; E: Loc. LL, half load, 20 m/h; F: Loc. L, full load, 20 m/h

DOCUMENT CONTROL DATA - R & D		
<i>Security classification of title, body of abstract and indexing annotation must be entered when the overall report is classified</i>		
1. ORIGINATING ACTIVITY (Corporate author) Naval Research Laboratory Washington, D.C. 20390		2a. REPORT SECURITY CLASSIFICATION <b>UNCLASSIFIED</b>
		2b. GROUP
3. REPORT TITLE <b>MEASUREMENT AND ANALYSIS OF ACCELERATION ENVIRONMENTS GENERATED BY NRL ROUGH ROAD SIMULATOR</b>		
4. DESCRIPTIVE NOTES (Type of report and inclusive dates) <b>This is a final report on this phase of the problem.</b>		
5. AUTHOR(S) (First name, middle initial, last name)  Edward W. Clements		
6. REPORT DATE <b>February 1970</b>	7a. TOTAL NO. OF PAGES <b>60</b>	7b. NO. OF REFS <b>8</b>
8a. CONTRACT OR GRANT NO. <b>NRL Problems F03-02 and F02-13</b>	9a. ORIGINATOR'S REPORT NUMBER(S)  <b>NRL Memorandum Report 2097</b>	
b. PROJECT NO.		
c.	9b. OTHER REPORT NO(S) (Any other numbers that may be assigned this report)	
d.		
10. DISTRIBUTION STATEMENT  <b>This document has been approved for public release and sale; its distribution is unlimited.</b>		
11. SUPPLEMENTARY NOTES		12. SPONSORING MILITARY ACTIVITY <b>Office of Naval Research and Naval Ship Systems Command Department of the Navy, Washington, D.C.</b>
13. ABSTRACT <p>The NRL Rough Road Simulator is a device for determining the resistance of military equipments to damage by the mechanical environments arising from ground transportation. Rough terrain is simulated by presenting a contoured surface moving at controlled speed to the wheels of a tethered vehicle which provides the appropriate mechanical interface between the terrain and the equipment under test. The output motions generated at the machine-equipment interface are of a quasi-random, vibratory nature, and consist of the rigid-body motions of the vehicle and its suspension system and the elastic motions of the vehicle's structure.</p> <p>The measurement and the analysis instrumentation system for such motions must extend the capability of a random vibration instrumentation system to very low frequencies, and in addition possess a high dynamic range capability, since collisions between adjacent structural components of the vehicle may produce local motions of a shock-like nature. A suitable instrumentation system has been assembled, and has provided a representative description of the output motions generated by the Rough Road Simulator and the influence of them of variations in some of the test conditions.</p> <p>The output motions studied were those produced with a Type M35 6x6 truck as the tethered vehicle. Acceleration waveforms were recorded at various points of the truck's cargo space for several equivalent truck speeds, and with dead-weight loads approximating its full rated capacity (5,000 lb), half of rated capacity, and without load. Data are presented in</p> <p style="text-align: right;">(continued)</p>		

14 KEY WORDS	LINK A		LINK B		LINK C	
	ROLE	WT	ROLE	WT	ROLE	WT
Reliability Transportation Environmental test Rough Road Simulator						
<p>terms of power spectral densities and rms acceleration to permit comparison of the motions at the various locations and to indicate how the motions themselves and the relationships between them are altered by changes in equivalent truck speed and payload.</p>						